



Model Error Resolution Document

QA: QA
Page 1 of 49

Complete only applicable items.

1. Document Number: MDL-NBS-HS-000006	2. Revision/Addendum: 03/01	3. ERD: 04
4. Title: UZ Flow Models and Submodels	5. No. of Pages Attached: 48	

6. Description of and Justification for Change (Identify affected pages, applicable CRs and TBVs):

The following evaluations are posted to address the conditions identified in CR-11715, CR-11762, CR-11796, and CR-12866 associated with *UZ Flow Models and Submodels* (MDL-NBS-HS-000006 REV 03 AD 01). A justification for no impact to the results or conclusions of *UZ Flow Models and Submodels* is included. See attached for detailed responses to each CR resolution. The condition related to a statistical value (coefficient of variation) for the post-10k infiltration rates (CR-12048), as indicated in the MGT-PRO-004.1-R0 evaluation form for this work, has been addressed in ERD 03 for *UZ Flow Models and Submodels*.

CR-11715 concerns the water table temperature used for the ambient thermal model. Calibration of the water table temperatures was performed to optimize the fit of the UZ ambient thermal model under a given infiltration rate. This calibration is inconsistent with the current use of the ambient thermal model as an independent assessment of infiltration rates. CR-11762 concerns the identification of pore-water chloride data as indirect input when used as direct input for the chloride model and addresses the qualification status of the chloride data used. CR-11796 concerns an erroneous cross-reference that should have been a reference to an external document. CR-12866 concerns the use of thermal properties data associated with a superseded report as direct input, without providing the required justification.

The changes to the main report are:

- (1) The analysis for CR-11715 adds Appendix J and corrects the DTN source information for Figures 6.3-2 through 6.3-6, 6.5-1 through 6.5-4, 6.5-6, 6.5-7, 6.5-8, 6.5-10, and 6.5-11 and provides corrections to Table 4.1-1. Also, corrections to Figures 6.5-1, 6.5-3, and 6.5-7 and text in Sections 6.3.3, 6.8.3, and Appendix G, Section G.1 are provided.
- (2) The analysis for CR-11762 adds Appendix K and provides corrections to Table 6.5-1.
- (3) The analysis for CR-11796 corrects Section 6.1.2. (Appendix L)
- (4) The analysis for CR-12866 provides a justification for the use of superseded product output LB0210THRMLPRP.001 in Table 4-1 (Appendix M)
- (5) The DIRS report has been updated to reflect changes made in this ERD.

	Printed Name	Signature	Date
7. Checker	Charles Haukwa		03/26/2009
8. QCS/QA Reviewer	Sounia Darnell		03/26/2009
9. Originator	David Sassani for Palmer Vaughn for 2 Jim Houseworth / Hui-Hai Liu		3/26/2009 / 3/26/2009
10. Responsible Manager	Palmer Vaughn Ernest Hardin		3/26/09

APPENDIX J
CR 11715 EVALUATION

J1 Background Information for CR-11715

In the original development of the water table temperature map in *UZ Flow Models and Submodels* (BSC 2001 [DIRS 158726] Section 6.3.2), water table temperatures over the ambient thermal model domain were first interpolated from the measured values of temperature in numerous boreholes at 730 m elevation. For cases where the borehole temperature measurements did not extend down to 730 m, temperatures at this elevation were estimated by linear extrapolation. Following this, water table temperatures were adjusted such that the predicted temperatures provided a best fit to the qualified temperature measurements in boreholes (qualified temperature boreholes: NRG-6, NRG-7a, SD-12 UZ#4, UZ#5 and UZ-7a). This calibration step was performed using the present-day mean infiltration map given in DTN: GS000399991221.002 [DIRS 147022]. This infiltration map is an output of the previous infiltration model (INFIL) documented in *Simulation of Net Infiltration for Present-Day and Potential Future Climates* (BSC 2004 [DIRS 170007]), which has been superseded by a new infiltration model (MASSIF) as described in REV01 AD01 of the same report (SNL 2008 [DIRS 182145]). The ambient thermal model is used as an independent method to assess infiltration rates. Therefore, calibration of the water table temperatures using any particular infiltration or percolation rates to optimize the fit between predicted and measured borehole temperatures is inconsistent with the current usage of the ambient temperature model. CR-11715 concerns this inconsistency associated with using the calibrated water table temperature map.

In this ERD, water table temperatures are interpolated directly from the water table measurements without calibration to model results. The revised water table temperature map is then used as a boundary condition for the ambient thermal model. The revised temperature results are used for re-assessing infiltration rates as documented in Section 6.8 of the main report (MDL-NBS-HS-000006 REV 03 AD 01 [DIRS 184614]).

J2 Inputs and/or Software

J2.1 Data

Corrections to direct inputs used in the main report and/or used in this ERD are listed in Table J-1. The items in Table J-1 associated with Appendices J, K, L, and M are contained in this ERD. The items in Table J-1 associated with Section 6 or Appendices D, G, or I are part of the main report. This table adds new entries or corrects corresponding entries in Table 4-1 of the main report.

Table J-1. Direct Inputs

DTN	Location in this Report			Description
	Section(s)	Figure(s)	Table(s)	
GS950208312232.003 [DIRS 105572]	6.3.2, 6.3.3, 6.8.6.1, G.1, I-3.1	6.3-2		Temperature measurements from borehole USW NRG-6. Surface temperatures for boreholes USW NRG-6 and USW NRG-7a.
GS031208312232.005 [DIRS 179284]	6.3.3, 6.8.6.1, G.1, I-3.1	6.2-4, 6.3-3 to 6.3-6		Temperature measurements from boreholes USW NRG-7a, USW SD-12, USW UZ-7a, UE-25 UZ #5
GS031208312232.004 [DIRS 182187]	6.3.3, I-3.1			Temperature measurements from boreholes USW NRG-7a, USW SD-12, USW UZ-7a, UE-25 UZ #5
GS031208312232.003 [DIRS 171287]	I-3.1	6.2-4, D.1-5	6.2-1	In situ water potential measurement in SD-12 and temperature data in Boreholes NRG-6, NRG-7a, SD-12 UZ#4, UZ#5, and UZ-7a
GS031208312232.007 [DIRS 178751] GS031208312232.006 [DIRS 182186]	I-3.1			Temperature data in Boreholes NRG-6, NRG-7a, SD-12 UZ#5, and UZ-7a
MO9906GPS98410.000 [DIRS 109059]	J3.4, J3.5			Borehole locations and ground surface elevations
GS010708312272.002 [DIRS 156375]	K2, K3	6.5-2, 6.5-6, 6.5-7, 6.5-11, J-15	6.5-1, K-1	Chloride concentration data from boreholes USW NRG-6, NRG77a, UZ-14 and UZ-N55, and UE-25 UZ#16
GS961108312271.002 [DIRS 121708]	K2, K3	6.5-1, 6.5-2, 6.5-3, 6.5-7, 6.5-8, J-15, J- 16, J-17	6.5-1, K-1	Chloride concentration data from boreholes USW NRG-6, USW NRG-7A, USW SD-7, USW SD-9, and USW SD-12, USW UZ-14.
GS000608312271.001 [DIRS 153407]	K2, K3	6.5-1, 6.5-8, J- 17	6.5-1, K-1	Chloride concentration data from boreholes USW SD-7 and USW SD-12.
GS970908312271.003 [DIRS 111467]	K2, K3	6.5-1, 6.5-3, 6.5-8, J-16, J- 17	6.5-1, K-1	Chloride concentration data from boreholes USW SD-7, USW SD-9 and USW SD-12.
GS981008312272.004 [DIRS 153677]	K2, K3	6.5-1, 6.5-7, 6.5-8, 6.5-10, J-17	6.5-1, K-1	Chloride concentration data from boreholes USW WT-24, USW UZ-7A, USW SD-6, USW SD-7, and USW SD-12
GS990208312272.001 [DIRS 146134]		6.5-2, 6.5-11	6.5-1, K-1	Chloride concentration data from USW UZ-14 and UE-25 UZ#16
LAJF831222AQ98.011 [DIRS 145402]	J3.5	6.5-2, 6.5-3, 6.5-6, 6.5-7, 6.5-8, 6.5-9, 6.5-11, J-15, J-16	6.5-1, K-1	Chloride concentration data from boreholes USW NRG-6, USW NRG-7A, USW SD-7, USW SD-9, USW UZ-14, USW UZ#16, USW WT-24, USW G-2.

Table J-1. Direct Inputs (Continued)

DTN	Location in this Report			Description
	Section(s)	Figure(s)	Table(s)	
GS020408312272.003 [DIRS 160899]	J3.6	6.5-3, 6.5-4, 6.5-7, J-15, J- 16	6.5-1, K-1	Chloride concentration data from boreholes USW SD-9 and USW NRG-7A and the ECRB.
LA0002JF12213U.002 [DIRS 156281]		6.5-4, 6.5-5	6.5-1, K-1	Chloride concentration data from the ECRB and ESF
LA9909JF831222.004 [DIRS 145598]		6.5-4	6.5-1, K-1	Chloride concentration data from the ECRB
GS961108312261.006 [DIRS 107293]		6.5-5	6.5-1, K-1	Chloride concentration data from the ESF
LA9909JF831222.010 [DIRS 122733]		6.5-5	6.5-1, K-1	Chloride concentration data from the ESF

J2.2 Software

The software and routines used in the modeling study of this report are listed in Table J-2. These codes are appropriate for the intended application and were used strictly within the range of validation. These codes were obtained from Software Configuration Management in accordance with IM-PRO-003, *Software Management*.

Table J-2. Software

Software Name, Codes	Version	Software Tracking Number (STN)	DIRS Reference Number	Operating Environment (Platform/Operating System)
TOPTMP_V0.f	1	10224-1.0-00	[DIRS 147030]	Dec Alpha/OSF1 V4.0
GET_TEMP_V0.f	1	10222-1.0-00	[DIRS 147027]	Dec Alpha/OSF1 V4.0
TOUGH2	1.6	10007-1.6-01	[DIRS 161491]	Dec Alpha/OSF1 V4.0, PC-DOS Window98

Standard spreadsheets and graphical display using Microsoft ® Excel 2003 and graphical display using Tecplot V7.0 are documented according to SCI-PRO-006.

J3 Analysis

J3.1 Development of Water Table Temperature Data at Boreholes

As stated in section J1, a new water table temperature map is developed that is independent of any infiltration model output. This is performed using measured water table temperature data and interpolation methods suitable for spatially-dependent information. In this section, the method for evaluating water table temperatures at boreholes with temperature measurements that extend to or below the water table is presented.

The water table temperatures used in the ambient thermal model have been analyzed using the temperature data in DTN: GS950408318523.001 [DIRS 107244] documented in the report by Sass et al. (1988 [DIRS 100644]) and the water table elevation data in DTN:

MO0106RIB00038.001 [DIRS 155631]. The temperature data was measured at 40 borehole locations and the water table elevation data was taken at 85 borehole locations. Both water table elevation and temperature data are found for 28 of these boreholes, with temperature data above and below water table in 26 out of the 28. At one borehole (UE-25 WT #18) the temperature measurements came to within 17 feet of the water table. For this borehole, the water table temperature is extrapolated and included in the set of measured water table temperatures. This gives a total of 27 water table temperature measurements (see DTN: LB0804WTMPCLGL.000 "measured water table elevations and temperatures.xls").

The temperature data is given as a function of borehole depth in DTN: GS950408318523.001 [DIRS 107244]. Therefore, water table elevations given in DTN: MO0106RIB00038.001 [DIRS 155631] must be converted to borehole depth to estimate the temperature at the water table. The water table elevations were converted to depth at each borehole using the ground elevation available in DTN: MO9906GPS98410.000 [DIRS 109059] (see DTN: LB0804WTMPCLGL.000, files "measured water table elevations and temperatures.xls"). The temperature data from approximately 600 feet below the surface to the water table was plotted as a function of depth for each borehole and a curve fit through this data was computed. The functional form of the curve fit was a second order polynomial. The curve fit was then used to estimate the water table temperature for the borehole using the depth to the water table. This then gives the basic water-table temperature data at the measurement boreholes to be used for establishing temperatures at the lower boundary of the ambient temperature numerical model (see DTN: LB0804WTMPCLGL.000, file "Borehole temperatures.xls").

J3.2 Development of the Temperature Semi-Variogram at the Water Table

Water table temperatures needed to be interpolated over the domain of the ambient thermal model at the nodal points of the bottom boundary of the numerical grid. This interpolation was performed using the geostatistical methodology called kriging. The kriging analysis begins with evaluating the spatial correlation present in the data in terms of a semi-variogram, which is defined as (Journal and Huijbregts 1978, page 31 [DIRS 102898]),

$$\gamma(x_1, x_2) = \frac{1}{2} \text{Var} \{T(x_1) - T(x_2)\} \quad (\text{Eq. J-1})$$

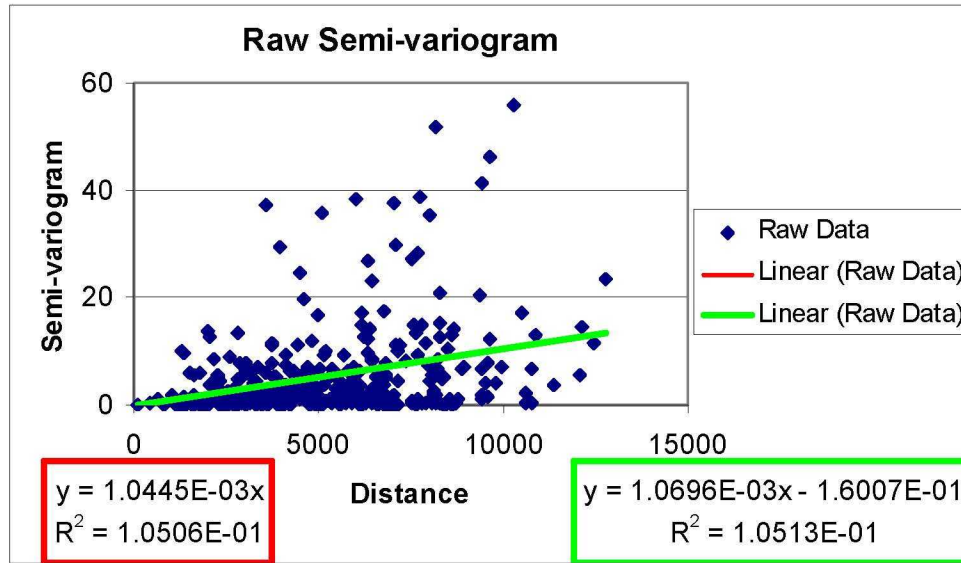
where the operator *Var* stands for the variance of the random spatial function defined by the temperature, *T*, and *x*₁ and *x*₂ are spatial coordinates. Under the assumption of stationarity, in which the random function only depends on the difference in spatial coordinates, the semi-variogram may be expressed as (Journal and Huijbregts 1978, page 32 [DIRS 102898]),

$$\gamma(h) = \frac{1}{2} \text{Var} \{T(x+h) - T(x)\} \quad (\text{Eq. J-2})$$

The water table temperature data were analyzed using this methodology, resulting in a tabulation of the semi-variogram value and distance for each borehole pair. Denote the water table temperatures for boreholes *i* and *j* as *T*_{*i*} and *T*_{*j*}, respectively, with distance *h*_{*ij*}

$$\gamma(h_{ij}) = \frac{1}{2} [T_i - T_j]^2 \tag{Eq. J-3}$$

for each borehole pair. Given 27 boreholes with temperature data at the water table, there are 351 borehole pairs. The resulting semi-variogram is shown in Figure J-1.

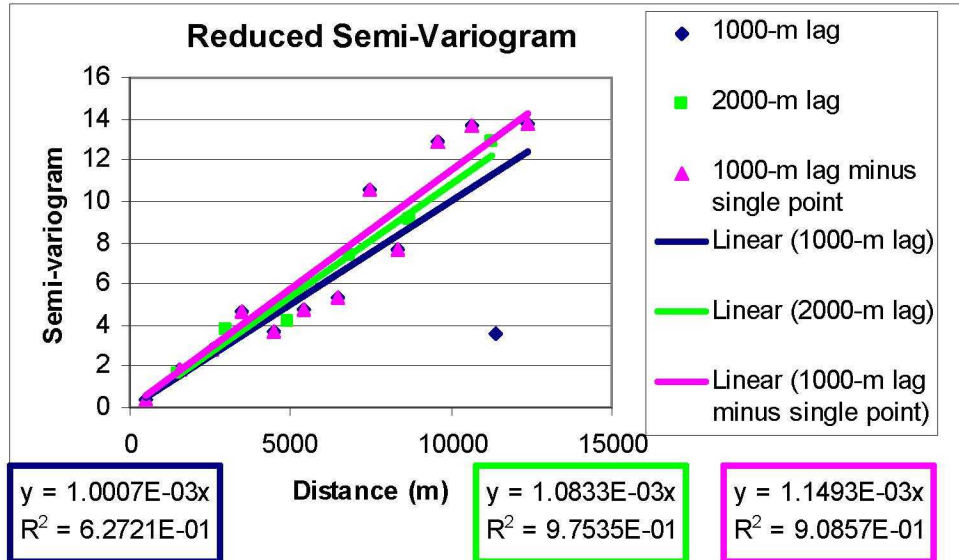


Source: DTN: LB0804WTMPCLGL.000

NOTE: Both linear fits (red and green) overlap in the figure. For both linear fits, Semi-variogram = $y = \gamma(h)$ and Distance = $x = h$.

Figure J-1. Raw Semi-Variogram of the Temperature Data

The data was fit with a linear model and Figure J-1 shows that the fit constrained to go through the origin is nearly identical to a general linear fit. A linear model was used due to the lack of information about the spatial correlation and the general scatter of the data. The data was also binned into 1000-m and 2000-m lag sections and averaged, as shown in Figure J-2. The averaged data over 1000-m and 2000-m lags appear to follow a linear model with no apparent sill. The effects of this on the linear fit of the semi-variogram are minimal. The "minus single point" case is where the point that falls off the trend for the 1000-m lag is removed from the fit. This point represents a bin with only one data point in the bin, therefore, the average for this bin is probably not representative. Given the small variation in slopes of the different fits and the arbitrary selections of lag spacing of the bins for the reduced semi-variograms, the fit to the raw semi-variogram data is used for kriging interpolation (see DTN: LB0804WTMPCLGL.000, "Variogram.xls").



Source: DTN: LB0804WTMPCLGL.000

NOTE: For all linear fits, Semi-variogram = $y = \gamma(h)$ and Distance = $x = h$.

Figure J-2. Semi-Variogram Data Binned into 1000-m and 2000-m Lags

Kriging Interpolation of Temperatures at the Water Table

The kriging method implemented is presented in Journel and Huijbregts (1978) [DIRS 102898], Section V.A.1). This method uses a weighted linear average of the measured values to determine an interpolated value, i.e.,

$$T(V) = \sum_{\beta} \lambda_{\beta} T_{\beta} \tag{Eq. J-4}$$

where $T(V)$ is the interpolated temperature, T_{β} are the measured water table temperatures, and λ_{β} are the weights for the β^{th} measurement.

The equations used to determine the weights are Equations V.3 of Journel and Huijbregts (1978) [DIRS 102898]. These equations are,

$$\sum_{\beta} \lambda_{\beta} \bar{\gamma}(v_{\alpha}, v_{\beta}) + \mu = \bar{\gamma}(v_{\alpha}, V) \tag{Eq. J-5}$$

$$\sum_{\beta} \lambda_{\beta} = 1 \tag{Eq. J-6}$$

where, v_{α} and v_{β} are temperature measurement locations, V is the interpolation location and μ is a Lagrange multiplier parameter for minimizing the estimation variance. In this case, there are 27 measured temperatures. Equations (J-5) and (J-6) comprise 28 linear equations that can be solved for the 27 weights, λ_{β} , and the Lagrange parameter.

Once these parameters are determined, the estimation variance at the interpolation point may be computed from (Journal and Huijbregts, 1978 [DIRS 102898], Section V.A.1)

$$\sigma_K^2 = \sum_{\alpha} \lambda_{\alpha} \bar{\gamma}(v_{\alpha}, V) + \mu - \bar{\gamma}(V, V) \quad (\text{Eq. J-7})$$

Because the estimation is all done using point measurement data for point interpolations, the term $\bar{\gamma}(V, V)$ in the equation for the estimation variance is zero. Values of $\bar{\gamma}(v_{\alpha}, v_{\beta})$ and $\bar{\gamma}(v_{\alpha}, V)$ are determined from the model semi-variogram, $\bar{\gamma}(h) = 0.00010445h$, presented in Figure J-1, where h is the distance between measurement locations or between a measurement location and an interpolation location.

Equations (J-5) and (J-6) consist of a set of linear equations for λ_{β} and μ , and may be expressed in matrix form (Journal and Huijbregts 1978 [DIRS 102898], Equation V.4):

$$K\lambda = M2 \quad (\text{Eq. J-8})$$

where

$$\lambda = \begin{bmatrix} \lambda_1 \\ \lambda_2 \\ \cdot \\ \lambda_{\alpha} \\ \cdot \\ \lambda_{26} \\ \lambda_{27} \\ -\mu \end{bmatrix} \quad (\text{Eq. J-9})$$

$$M2 = \begin{bmatrix} \bar{\gamma}(v_1, V) \\ \bar{\gamma}(v_2, V) \\ \cdot \\ \bar{\gamma}(v_{\alpha}, V) \\ \cdot \\ \bar{\gamma}(v_{26}, V) \\ \bar{\gamma}(v_{27}, V) \\ 1 \end{bmatrix} \quad (\text{Eq. J-10})$$

and

$$K = \begin{bmatrix} \bar{\gamma}(v_1, v_1) \dots \bar{\gamma}(v_1, v_\beta) \dots \bar{\gamma}(v_1, v_{27}) & 1 \\ \bar{\gamma}(v_2, v_1) \dots \bar{\gamma}(v_2, v_\beta) \dots \bar{\gamma}(v_2, v_{27}) & 1 \\ \cdot & \cdot & \cdot & \cdot \\ \cdot & \cdot & \cdot & \cdot \\ \cdot & \cdot & \cdot & \cdot \\ \bar{\gamma}(v_\beta, v_1) \dots \bar{\gamma}(v_\beta, v_\beta) \dots \bar{\gamma}(v_\beta, v_{27}) & 1 \\ \cdot & \cdot & \cdot & \cdot \\ \cdot & \cdot & \cdot & \cdot \\ \cdot & \cdot & \cdot & \cdot \\ \bar{\gamma}(v_{26}, v_1) \dots \bar{\gamma}(v_{26}, v_\beta) \dots \bar{\gamma}(v_{26}, v_{27}) & 1 \\ \bar{\gamma}(v_{27}, v_1) \dots \bar{\gamma}(v_{27}, v_\beta) \dots \bar{\gamma}(v_{27}, v_{27}) & 1 \\ 1 & \dots & 1 & \dots & 1 & 0 \end{bmatrix} \quad (\text{Eq. J-11})$$

The solution to Equation (J-8) is,

$$\lambda = K^{-1}M2 \quad (\text{Eq. J-12})$$

The interpolation points are the 980 bottom grid nodes in the UZ ambient thermal model (Output DTN: LB0701UZMTHCAL.001). For interpolation onto 980 points, the matrix $M2$ may be expanded from a 28×1 matrix to a 28×980 matrix, resulting in a matrix λ that is 28×980 . Given this matrix size and the 256 cell field width limit in Microsoft® Excel 2003, it is more convenient to use the transpose of Equation (J-12), i.e.,

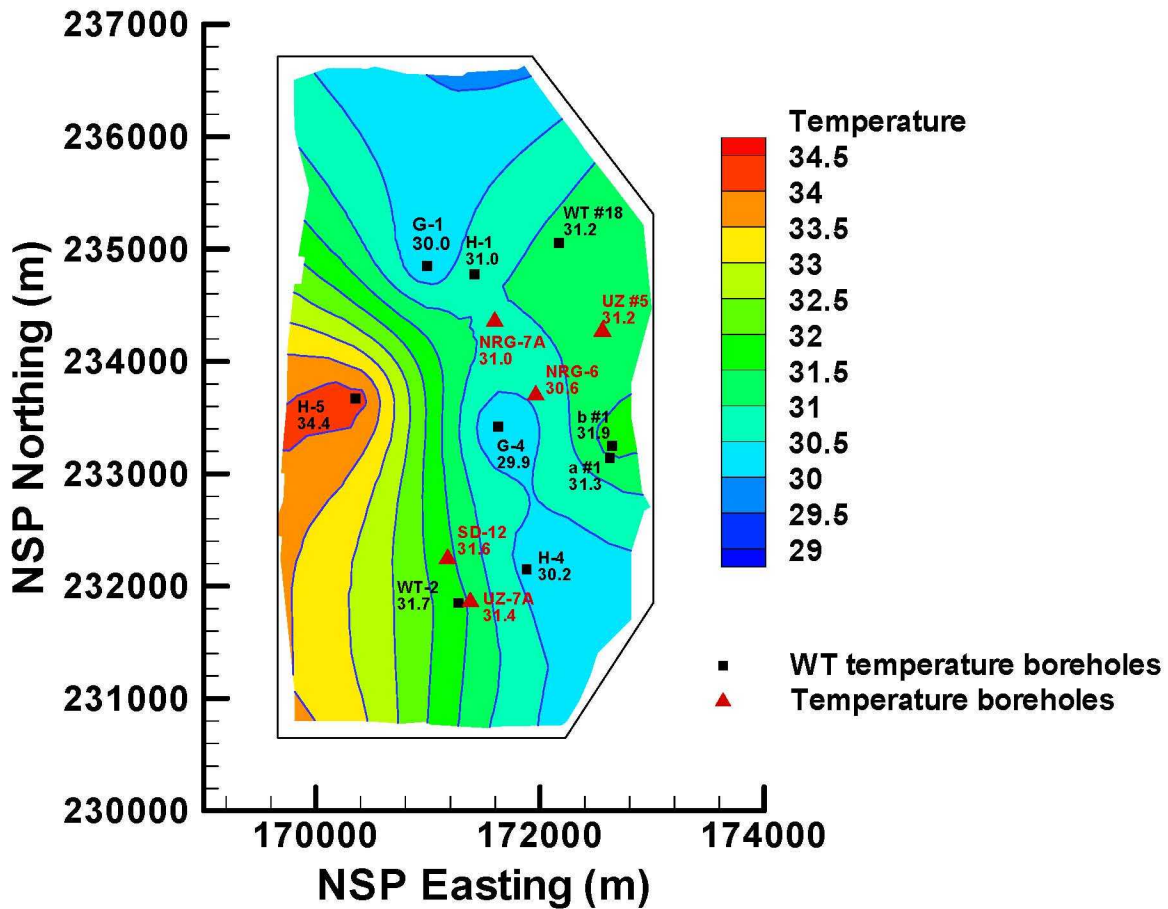
$$\lambda^T = M2^T (K^{-1})^T \quad (\text{Eq. J-13})$$

Because Microsoft® Excel 2003 can treat up to 65536 lines, Equation (J-13) could be used to compute all 980 sets of weights (λ^T) in one calculation. However, Excel is also limited in the number of cells in a given matrix (5461 cells) that may participate in matrix multiplication. Because of this limit, the matrix $M2^T$ is limited to 195 rows (which corresponds to 195 nodes at the water table) for a given interpolation calculation. Thus, Equation (J-13) is computed six times to generate the set of weights for each of the 980 points at the water table. Then Equation (J-4) is used to generate the mean interpolated temperatures and Equation (J-7) is used to generate the estimation variance at each node (see DTN: LB0804WTMPCLGL.000, file "Kriging.xls").

J3.3 Results

The results of the kriging interpolation are shown in Figure J-3 for the water table contour plot. All contour plots were generated using Tecplot V7.0-4.0. This was done using the Tecplot “triangulate” option using the water table temperature values, the model domain boundary, and a “triangle keep factor” of 0.25.

The water table temperature map in Figure J-3 is a direct interpolation of the water table temperature measurement data and therefore is not affected by calibration to infiltration model output, unlike Figure 6.3-7 of the main report. This water table temperature map is used in the following sections for ambient temperature calculations instead of the map shown in Figure 6.3-7 of the main report.



Sources: DTNs: GS950408318523.001 [DIRS 107244]; MO0106RIB00038.001 [DIRS 155631]; MO9906GPS98410.000 [DIRS 109059]

DTN: LB0804WTMPCLGL.000

NOTE: Water table temperature contours interpolated from the 27 borehole water table temperature measurements. Only 9 of the 27 boreholes are within the UZ ambient thermal model domain shown in the figure. Boreholes identified by black squares are water table temperature measurement boreholes. Boreholes identified by red triangles are boreholes used for temperature analyses of percolation flux. Water table temperatures at these boreholes are interpolated from the water table measurement borehole values. The contoured area corresponds to the ambient thermal model domain as shown in Figure 6.3-7 of the main report.

Figure J-3. Water Table Temperature Contour Plot

J3.4 Re-Analyses of Temperature

During the investigation of CR-11715, it was also discovered that Figures 6.3-2 through 6.3-6 show incorrect source DTN information. The DTN sources should be changed as follows: Figure 6.3-2, Source DTN: GS950208312232.003 [DIRS 105572]; Figures 6.3-3 through 6.3-6, Source DTN: GS031208312232.005 [DIRS 179284]. Also, the last sentence of the first paragraph of Section 6.3.3 should be changed to:

The initially estimated water table temperatures show a good match to the measurements through comparison with the qualified temperature data in boreholes NRG-6, NRG-7a, SD-12 UZ#4, UZ#5, and UZ-7A (DTNs: GS950208312232.003 [DIRS 105572] and GS031208312232.005 [DIRS 179284]).

During the investigation of CR-11715, it was discovered that the text in Sections 6.8 and Appendix G, Section G.1 stated an incorrect depth limitation for the temperature measurements used. The last sentence in the first paragraph of Section 6.8.3 should be changed to:

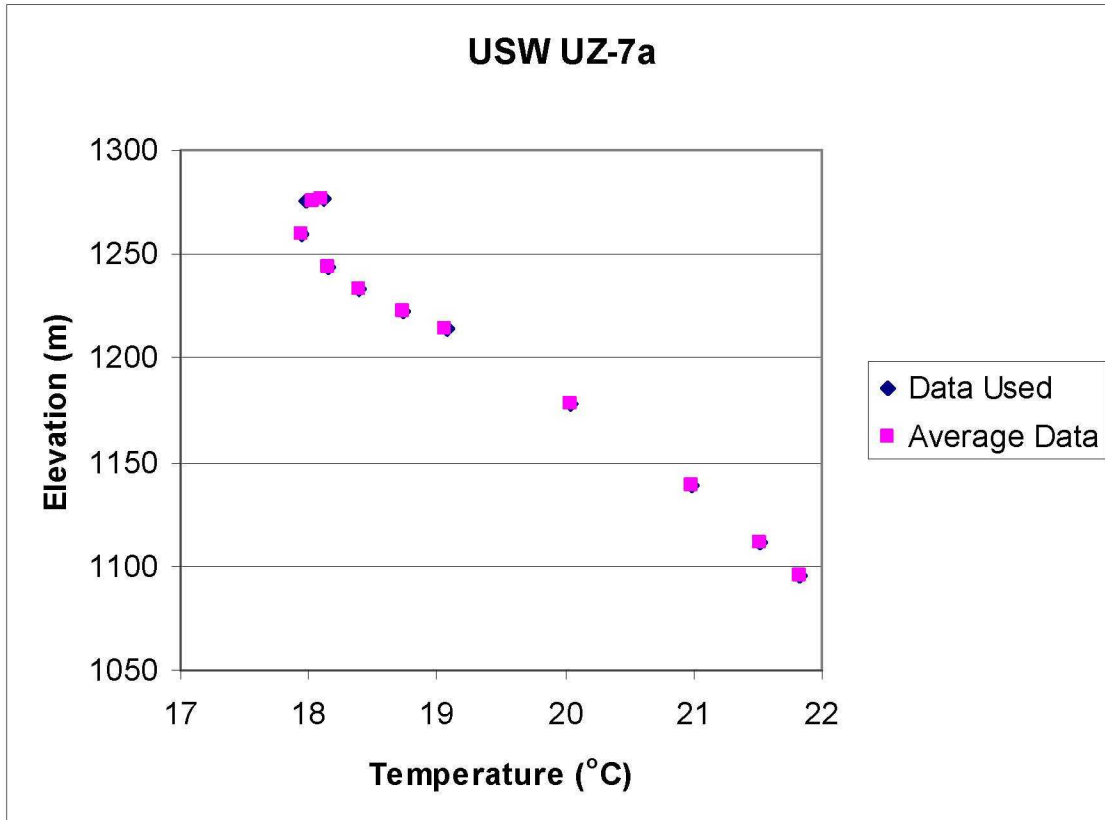
In this study, only measurements greater than 12 m below ground surface were considered. Even at a 12-m depth, the stability of the average temperature was sufficient for use in the analyses.

And in Section G.1, the second sentence on page G-3 should be changed to:

The temperature data less than 12 m from the ground surface are not considered due to greater uncertainty.

The data plotted in Figures 6.3-2 through 6.3-6 are a subset of the total temperature data recorded in these boreholes. Lengthy time-temperature histories are available at each measurement location in each of these five boreholes. Only a subset of these data is used in this ERD and in section 6.8 of the main report. To justify the use this subset of the total data, a comparison between the subset of data used and the average of all the data has been developed. Only data for temperatures at 12 m (40 ft) or greater depth are included in the comparison because temperature data at shallower depths are affected by diurnal and seasonal temperature variations. Note that the ambient thermal model uses a steady-state approximation that does not represent these variations. Temperature data used for the weighting factor analysis were also limited to locations 12 m (40 ft) or deeper. Note that temperature data are recorded versus depth from the borehole ground surface; therefore, to convert depth to elevation requires the ground surface elevation for each borehole. These values are available from DTN: MO9906GPS98410.000 [DIRS 109059].

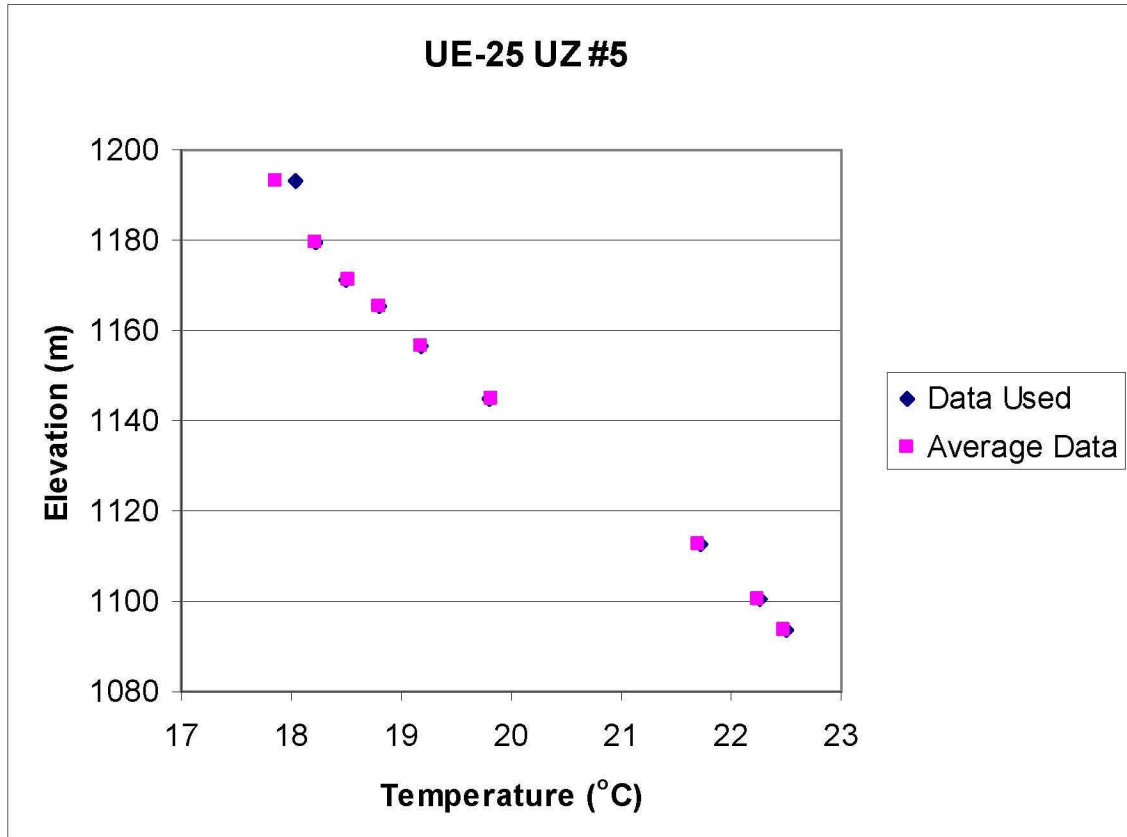
Figures J-4 through J-8 show the comparison of the data used for each of five boreholes and the average of all the data over time at each measurement location. The absolute value of temperature differences between the data used and total data averages are found to average about 0.02 degrees Celsius, with a standard deviation of 0.04 degrees Celsius and a maximum difference of less than 0.3 degrees Celsius. These temperature differences are much smaller than the differences in water table temperatures evaluated in Sections J3.1 to J3.3, which are shown to have little effect on the weighting factors. Therefore, the use of the subset of temperature data, as compared with the average of all the data, should have a negligible effect on the resulting weighting factors.



Sources: DTNs: GS031208312232.003 [DIRS 171287], GS031208312232.004 [DIRS 182187], GS031208312232.005 [DIRS 179284], GS031208312232.006 [DIRS 182186], GS031208312232.007 [DIRS 178751]

DTN: LB0804WTMPCLGL.000

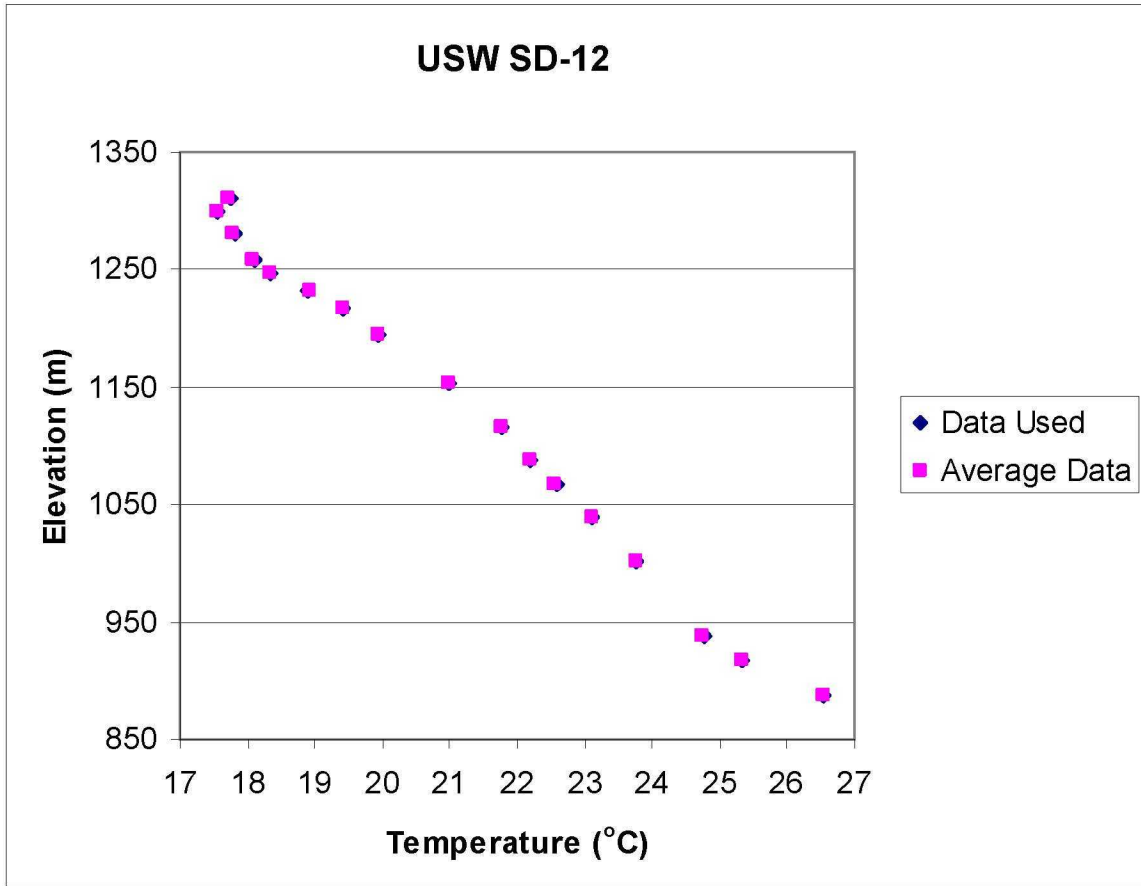
Figure J-4. Comparison of Temperature Data Used in the Weighting Factor Analysis with the Average of All Data at Each Measurement Location in Borehole USW UZ-7a



Sources: DTNs: GS031208312232.003 [DIRS 171287], GS031208312232.004 [DIRS 182187], GS031208312232.005 [DIRS 179284], GS031208312232.006 [DIRS 182186], GS031208312232.007 [DIRS 178751], GS951108312232.008 [DIRS 106756]

DTN: LB0804WTMPCGL.000

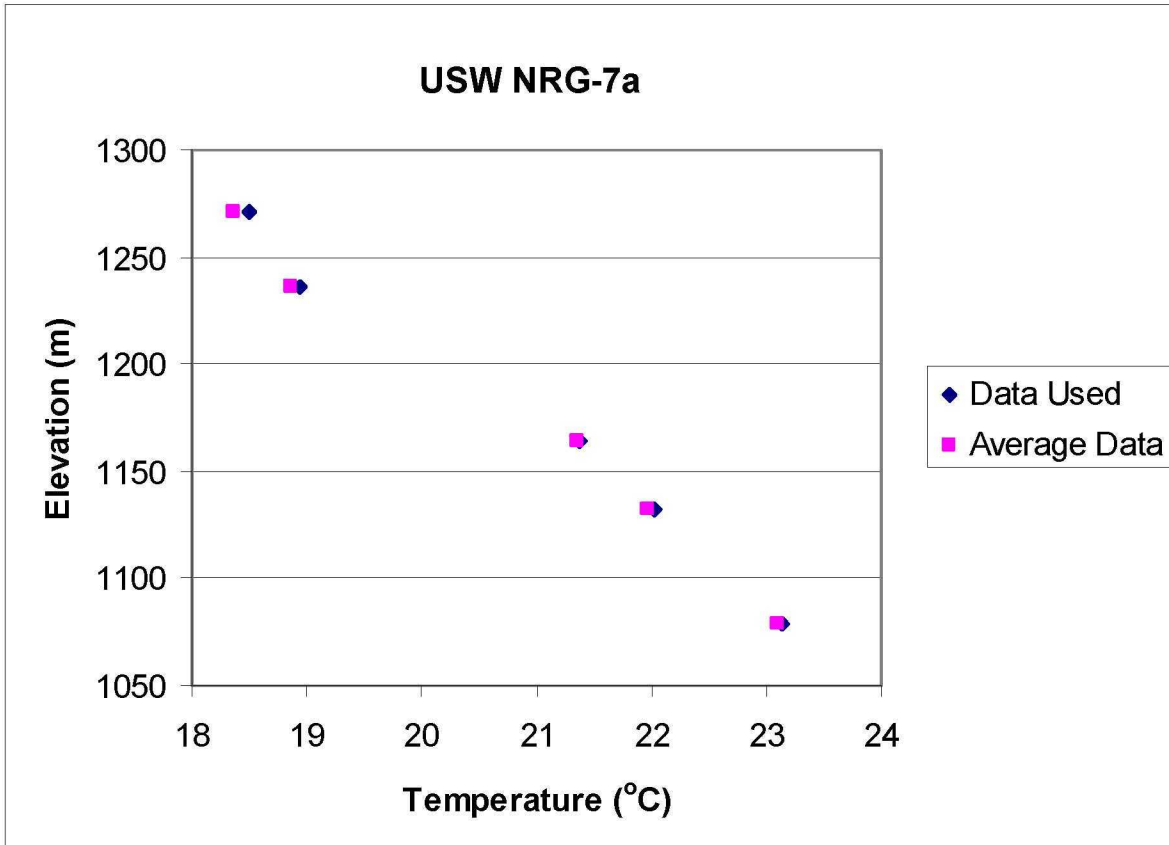
Figure J-5. Comparison of Temperature Data Used in the Weighting Factor Analysis with the Average of All Data at Each Measurement Location in Borehole UE-25 UZ #5



Sources: DTNs: GS031208312232.003 [DIRS 171287], GS031208312232.004 [DIRS 182187], GS031208312232.005 [DIRS 179284], GS031208312232.006 [DIRS 182186], GS031208312232.007 [DIRS 178751]

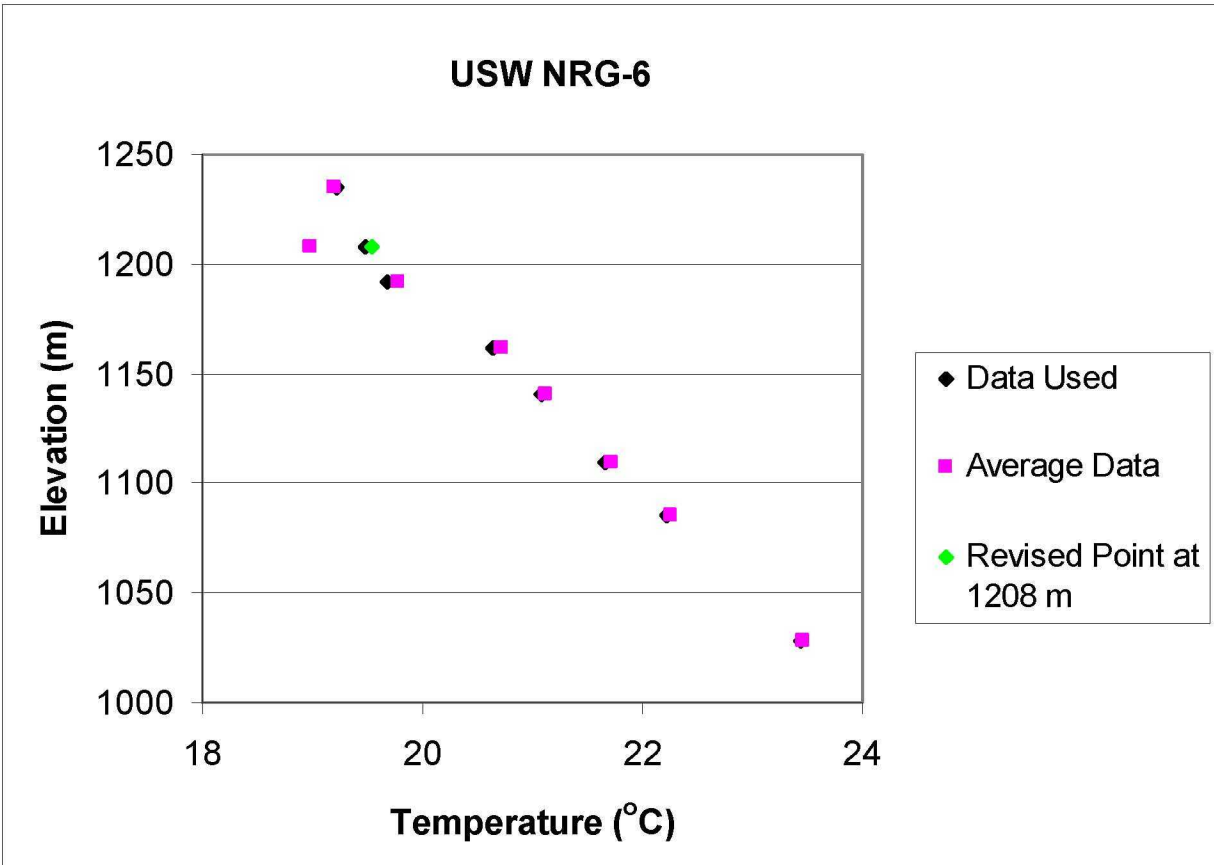
DTN: LB0804WTMPCGL.000

Figure J-6. Comparison of Temperature Data Used in the Weighting Factor Analysis with the Average of All Data at Each Measurement Location in Borehole USW SD-12



Sources: DTNs: GS031208312232.003 [DIRS 171287], GS031208312232.004 [DIRS 182187], GS031208312232.005 [DIRS 179284], GS031208312232.006 [DIRS 182186], GS031208312232.007 [DIRS 178751], GS950208312232.003 [DIRS 105572], GS951108312232.008 [DIRS 106756]
 DTN: LB0804WTMPCGL.000

Figure J-7. Comparison of Temperature Data Used in the Weighting Factor Analysis with the Average of All Data at Each Measurement Location in Borehole USW NRG-7a



Sources: DTNs: GS031208312232.003 [DIRS 171287], GS031208312232.006 [DIRS 182186], GS031208312232.007 [DIRS 178751], GS950208312232.003 [DIRS 105572], GS951108312232.008 [DIRS 106756]

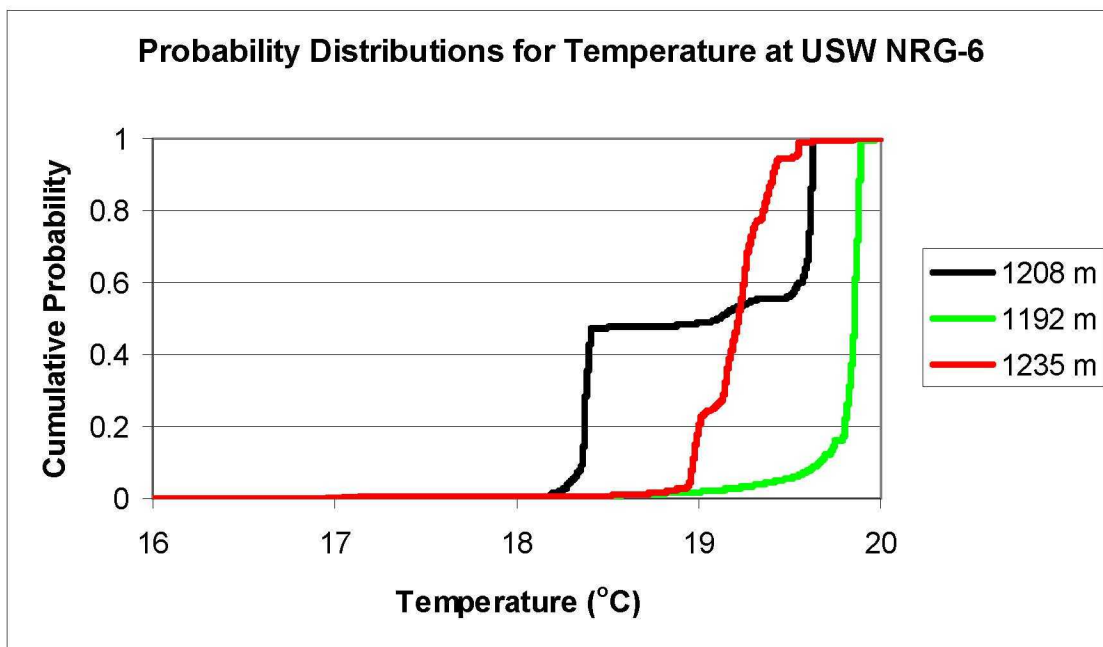
DTN: LB0804WTMPCGL.000

Figure J-8. Comparison of Temperature Data Used in the Weighting Factor Analysis with the Average of All Data at Each Measurement Location in Borehole USW NRG-6

One point in the profile for NRG-6 in Figure J-8, at an elevation of about 1208 m, was found to be anomalous. Figure J-9 shows the total distributions of temperature at three locations: at 1208 m and at locations immediately above and below this location where temperatures were recorded. As can be seen in Figure J-9, the distribution of temperatures at 1208 m shows a bimodal character unlike the distributions for temperature at locations above and below this point. The “normalized rank order” values on the ordinate of Figure J-9 represent the sequential rank order (from lowest to highest temperatures) divided by the total number of points plus one. There appears to be two equilibrium temperatures at the 1208 m elevation, however only the higher equilibrium temperature is consistent with an increase in temperature with depth. The cause of this behavior is unknown, but can be traced to two thermistors at this elevation in borehole NRG-6 that were not in agreement: thermistor THM741 (which gives the higher temperatures) and THM742 (which gives the lower temperatures). The temperature readings from the two thermistors were reasonably close during the first 18 days of data collection. The absolute value of the temperature differences averaged about 0.1 °C from the initial reading on 11/17/1994 through 12/4/1994 (DTN: GS950208312232.003 [DIRS 106756]). However, on

12/5/1994, the temperature reading from thermistor THM742 dropped from 19.3 °C to 18.2 °C in the span of about 3.5 hours while over the same time thermistor THM741 remained approximately constant at 19.2 °C. From that point forward (until the final measurement on 3/31/1998), the temperature reading from thermistor THM742 was approximately one degree lower than from thermistor THM741.

Because the increase in equilibrium temperature with depth is expected, an average of the data from 1208 m was taken for temperatures 19 degrees Celsius and above. This temperature cutoff was used because it lies about in the middle between the two equilibrium temperatures found in the distribution. The adjusted average temperature is also plotted on Figure J-8, which shows that this adjustment makes the temperature at 1208 m consistent with an increase in temperature with depth.



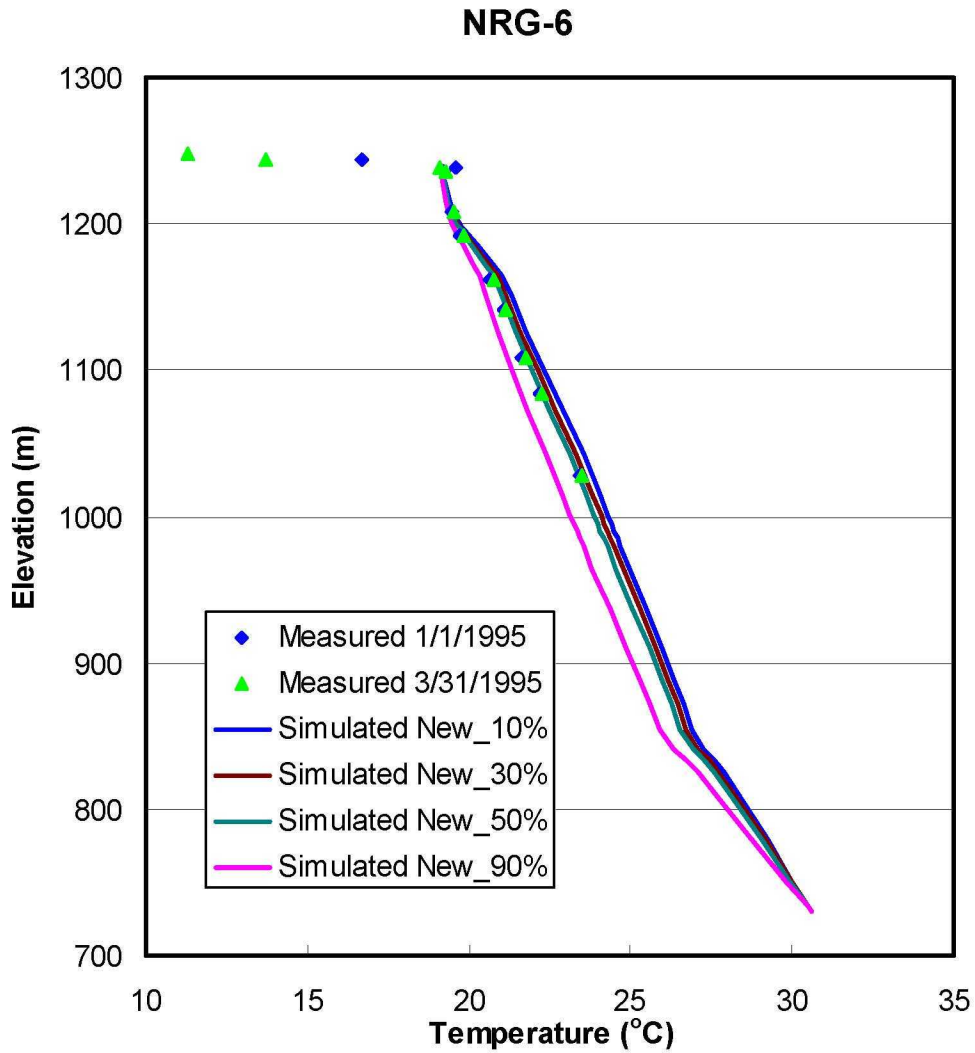
Sources: DTNs: GS031208312232.003 [DIRS 171287], GS031208312232.006 [DIRS 182186], GS031208312232.007 [DIRS 178751], GS950208312232.003 [DIRS 105572], GS951108312232.008 [DIRS 106756]

DTN: LB0804WTMPCLGL.000

Figure J-9. Comparison of Distributions for Temperature at Three Elevations in Borehole USW NRG-6

Using the interpolated temperatures at the water table described in Sections J3.1 to J3.3, the analyses of temperature in the unsaturated zone as described in Section 6.3 of the main report were repeated. As before, infiltration was defined for the simulations using DTN: SN0609T0502206.028 [DIRS 178753], thermal conductivities were taken from DTN: LB0210THRMLPRP.001 [DIRS 160799], the three-dimensional model grid was taken from LB0303THERMESH.001 [DIRS 165168], and results for assigning surface temperatures from DTN: LB0303THERMSIM.001 [DIRS 165167]. The temperature profiles from the simulations conducted in this ERD are shown in Figures J-10 through J-14, corresponding to Figures 6.3-2 through 6.3-6 in the main report.

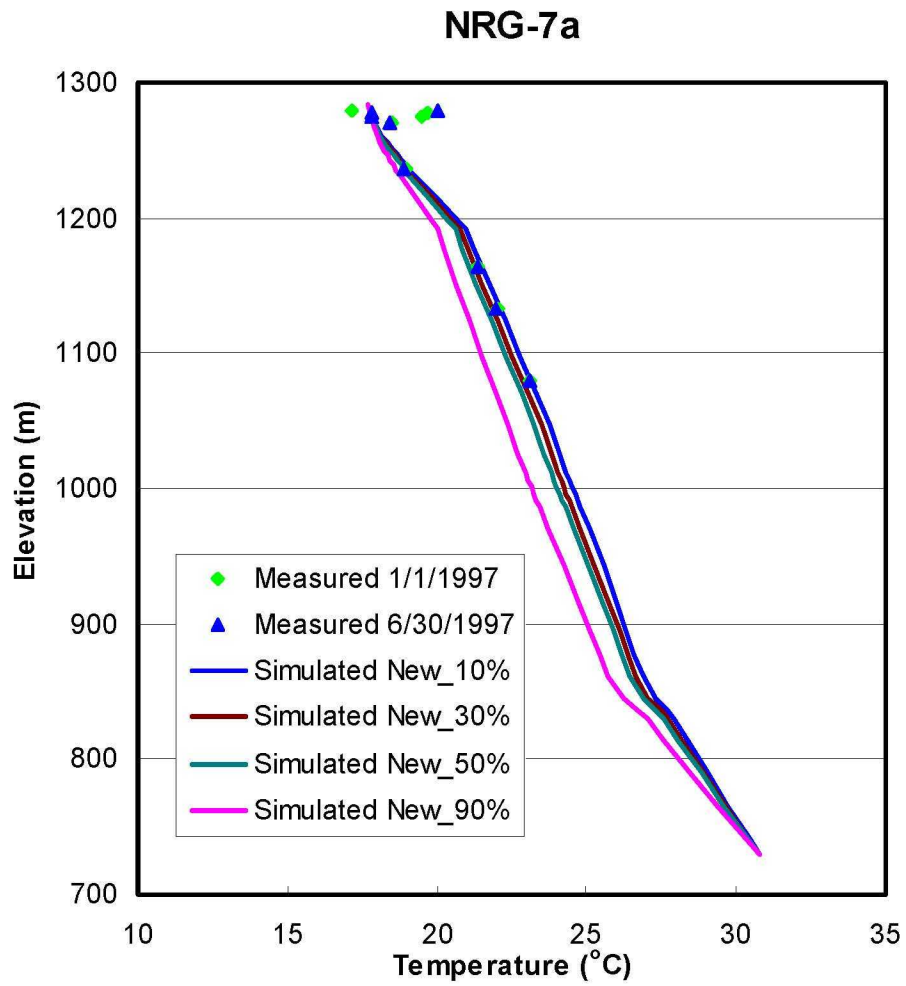
DTN: LB0210THRMLPRP.001 [DIRS 160799] was used for thermal conductivities in this ERD and is identified in the Technical Data Management System with the following statement: "THIS IS A HISTORIC TPO DTN AND SHOULD NOT BE USED IN LA PRODUCTS WITHOUT PA MANAGEMENT APPROVAL." The reason for using DTN: LB0210THRMLPRP.001 [DIRS 160799] for the thermal analysis in this ERD is that these thermal conductivities were used in the baseline thermal analysis, as shown in Table 4-1 of the parent report. Furthermore, the goal of the thermal sensitivity analysis presented in this ERD is to evaluate the sensitivity of the ambient thermal model results to the water table temperature boundary condition. Changing both thermal conductivities and the water table temperature boundary condition in the sensitivity analysis would make interpretation of the results ambiguous. Note that other thermal properties in DTN: LB0210THRMLPRP.001 [DIRS 160799] only affect the thermal energy content of the system and do not affect the steady-state solution for temperature. A separate analysis for CR-12866 is presented in this ERD to provide the technical justification for the use of DTN: LB0210THRMLPRP.001 [DIRS 160799] as direct input in the baseline analysis.



Source: DTN: GS950208312232.003 [DIRS 105572]

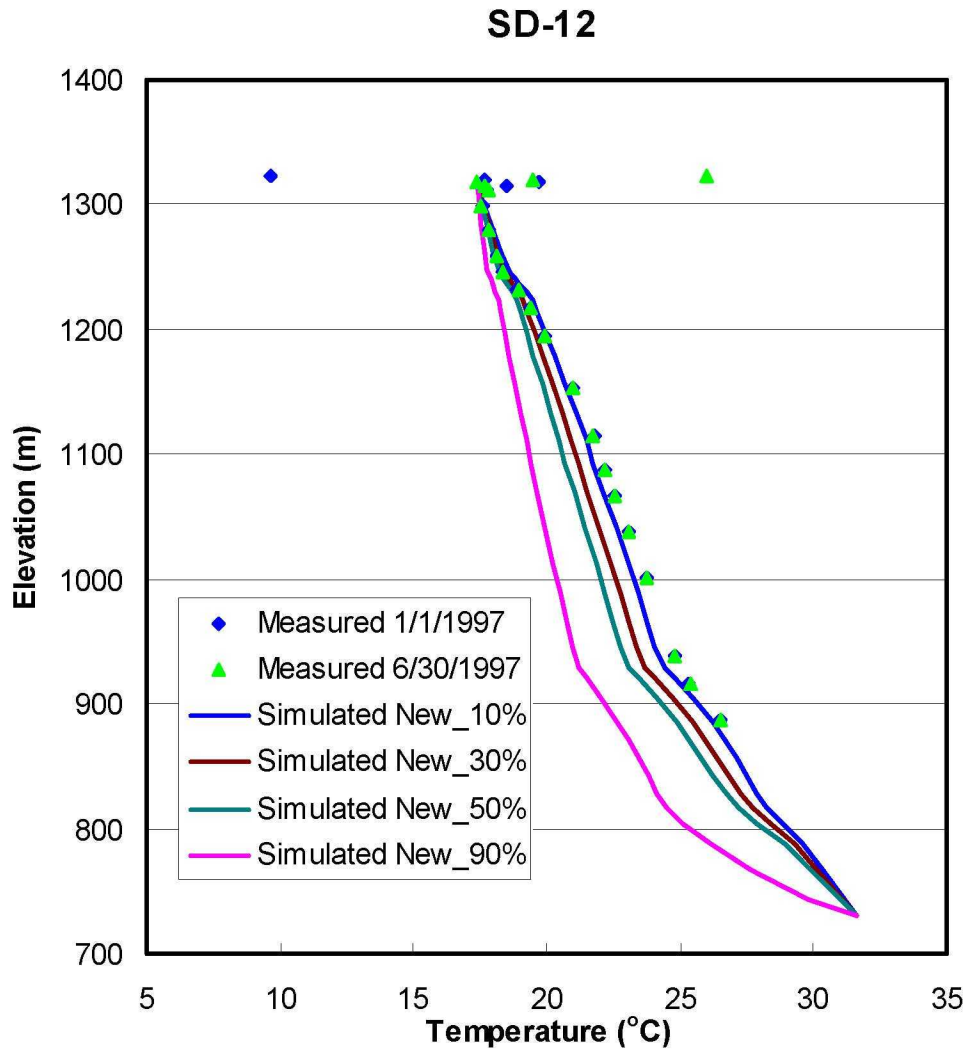
DTN: LB0803UZTHRUNS.001

Figure J-10. Comparisons between Measured and Modeled Ambient Temperature Profiles in Borehole NRG-6 for the Four Infiltration Maps of 10th, 30th, 50th and 90th Percentile Present-Day Infiltration Rate



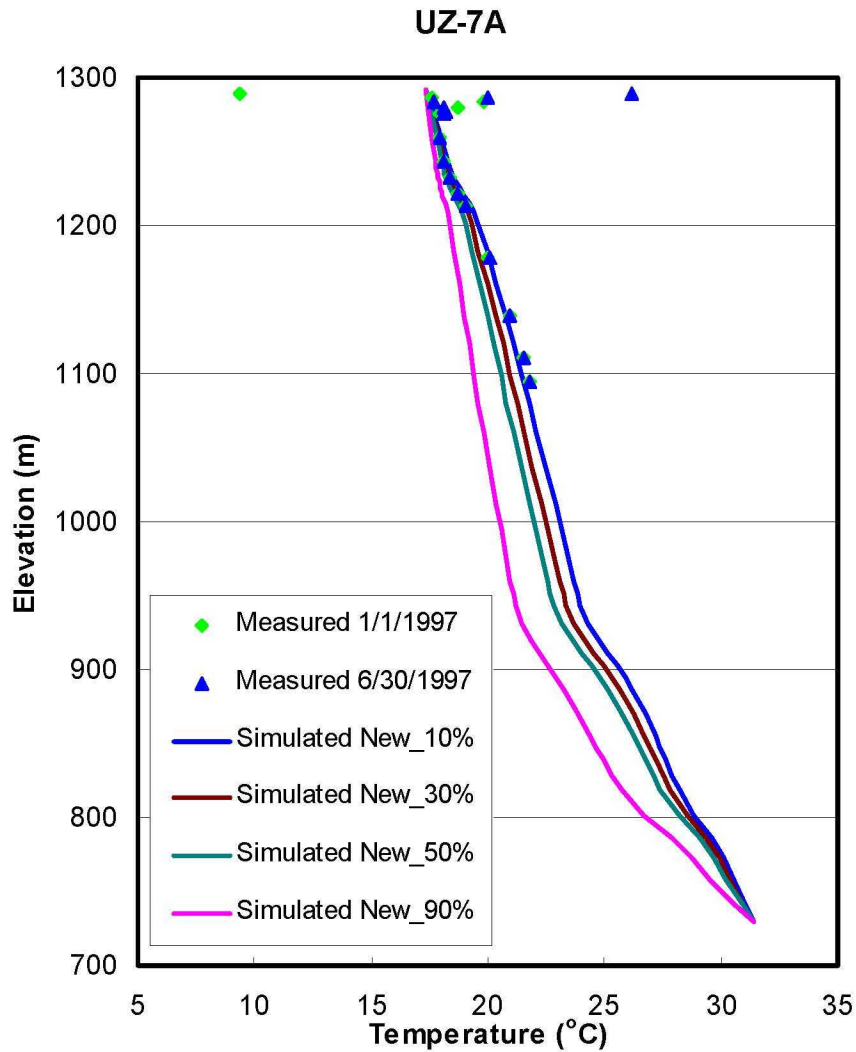
Source: DTN: GS031208312232.005 [DIRS 179284]
 DTN: LB0803UZTHRUNS.001

Figure J-11. Comparisons between Measured and Modeled Ambient Temperature Profiles in Borehole NRG-7A for the Four Infiltration Maps of 10th, 30th, 50th and 90th Percentile Present-Day Infiltration Rate



Source: DTN: GS031208312232.005 [DIRS 179284]
 DTN: LB0803UZTHRUNS.001

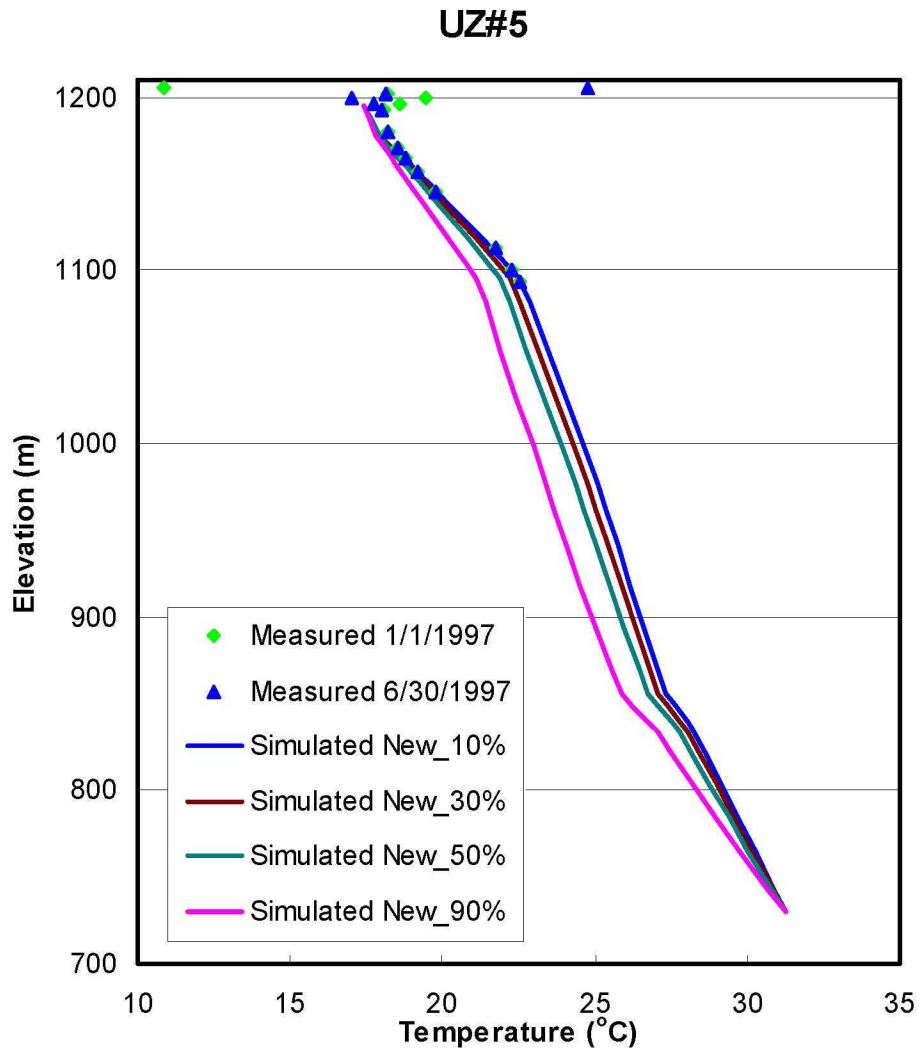
Figure J-12. Comparisons between Measured and Modeled Ambient Temperature Profiles in Borehole SD-12 for the Four Infiltration Maps of 10th, 30th, 50th and 90th Percentile Present-Day Infiltration Rate



Source: DTN: GS031208312232.005 [DIRS 179284

DTN: LB0803UZTHRUNS.001

Figure J-13. Comparisons between Measured and Modeled Ambient Temperature Profiles in Borehole UZ-7A for the Four Infiltration Maps of 10th, 30th, 50th and 90th Percentile Present-Day Infiltration Rate



Source: DTNs: GS031208312232.005 [DIRS 179284]

DTN: LB0803UZTHRUNS.001

Figure J-14. Comparisons between Measured and Modeled Ambient Temperature Profiles in Borehole UZ#5 for the Four Infiltration Maps of 10th, 30th, 50th and 90th Percentile Present-Day Mean Infiltration Rate

Table J-3 shows the average temperature residuals for each uncertainty case and borehole. As can be seen, at each location the minimum residual occurs for the same uncertainty cases as given in Table 6.3-2 of the main report.

Table J-3. Average Temperature Residuals Between Measured and Computed Values

Borehole	10th Percentile ^a	30th Percentile	50th Percentile	90th Percentile
UZ-7A	-0.44 ^b	-1.70	-2.83	-5.81
NRG-6	1.40	0.80	0.29 ^b	-1.60
NRG-7a	0.10 ^b	-0.73	-1.50	-3.88
SD-12	-0.64 ^b	-2.71	-4.38	-9.81
UZ#5	-0.77 ^b	-1.44	-2.16	-4.08

DTN: LB0804WTMPCLGL.000

^a Percentile infiltration map of present-day climate^b Minimum absolute residual case.

NOTE: Residual temperature takes average of percentage of difference between calculated and measured temperature relative to the calculated value (°C).

J3.5 Inclusion of Additional Chloride Data and Other Changes

Chloride analyses were performed in Section 6.5 of the main report to compare against measurements of pore-water chloride content taken from boreholes and the ESF and ECRB tunnels. All pore-water chloride data from the unsaturated zone were intended to be used in this analysis; however, several data sets were inadvertently not included. This section evaluates the impact of including this data in the analysis.

In addition to the data sets identified in Table 6.5-1 of the main report, appropriate chloride data were also available in DTNs: GS030408312272.002 [DIRS 165226], GS031008312272.008 [DIRS 166570], GS020808312272.004 [DIRS 166569], GS0703PA312272.001 [DIRS 182478], GS060908312272.004 [DIRS 179065], GS041108312272.005 [DIRS 178057], and GS011008312272.004 [DIRS 165859]. These DTNs contain chloride data for the ECRB, ESF, Alcove 5, Alcove 7, and boreholes NRG-7a, SD-6, SD-9, SD-12, and WT-24. Alcove 5 is the thermal test drift; note that data for Alcove 5 has not been included in the analyses for this ERD because of the potential effects of the heated drift test conducted in Alcove 5 on the pore-water chloride concentrations. Alcove 7 is the southern Ghost Dance Fault test drift and has been included in the analysis but does not appear on any figures. This data set is not displayed on figures because the ESF figure displays measured and computed chloride concentrations along the ESF and the data from Alcoves 7 is laterally offset from the ESF. Furthermore, data in DTN: GS020408312272.003 [DIRS 160899], although included in the original analyses, was not included in Figure 6.5-3 for chloride levels in borehole SD-9, Figure 6.5-4 for chloride levels in the ECRB, and Figure 6.5-7 for chloride levels in borehole NRG-7a. These data have been added to the figures presented below.

The locations where the chloride data were taken in DTNs GS030408312272.002 [DIRS 165226] and GS031008312272.008 [DIRS 166570] required additional information in some cases. The location of samples taken from borehole ESF-SAD-GTB#1 in Alcove 7 is given in SIT.20030514.0001 [DIRS 185752]. Locations of the ESF-THERMALK-017 and -019 are given in DTN: SN0606F3504502.024 [DIRS 185417] (Records package item MOL.20060731.0045). Locations of the ESF-NR-MS#3, #6, #8, #10, #11, and #15 are given in DTN: GS060308312272.001 [DIRS 176859] (records package item SIT.20030826.0001). Locations of the ESF-SR-MS#22 and #23 are given in DTN: GS060308312272.001 [DIRS 176859] (records

package item SIT.20030828.0002). The locations of the ESF-NR-MS#3 and #6 and the ESF-SR-MS#22 and #23 were given in terms of Nevada State Plane coordinates that were converted into ESF stations (i.e., distance along the ESF) using data relating these two position identification methods (DTN: MO08103DDRFTCD.001 [DIRS 185803]). The Nevada State Plane coordinates for borehole ESF-SAD-GTB#1 in Alcove 7 were used directly because these data were laterally offset from the ESF. The NSP coordinates in this case were used to identify the nearest UZ model cell for comparison with the data.

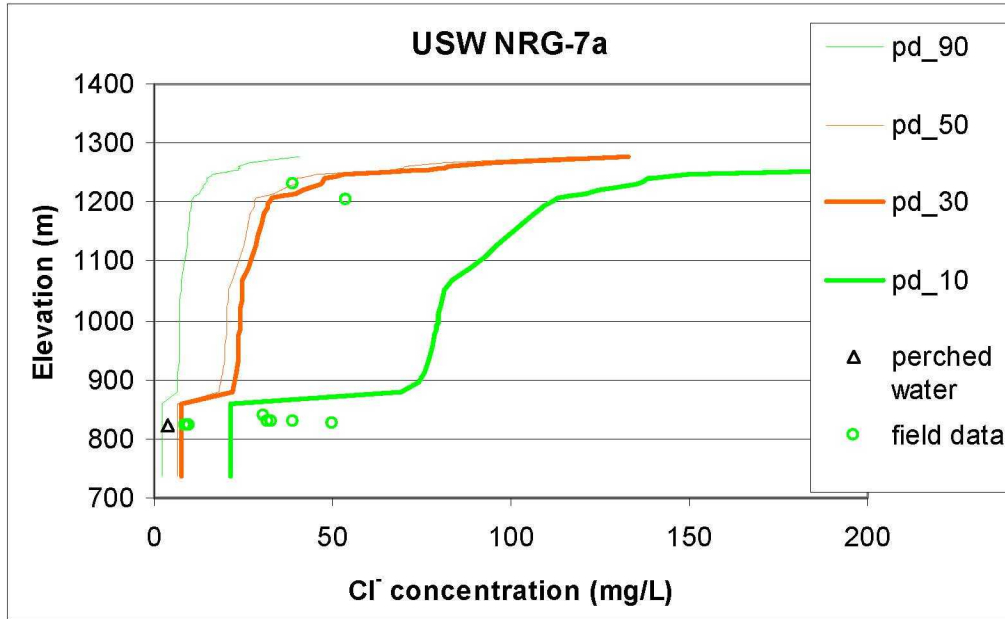
Most borehole elevations required to determine chloride sample elevations in boreholes were taken from DTN: MO9906GPS98410.000 [DIRS 109059]. Additional information is required for boreholes USW SD-6 and USW WT-24 beyond what is available in DTN: MO9906GPS98410.000 [DIRS 109059] for the elevations. Borehole elevation for USW SD-6 is from DTN: MO9912GSC99492.000 [DIRS 165922] and borehole elevation for USW WT-24 is from DTN: DTN: MO9905LUSWWT24.000 [DIRS 165921].

The depths of chloride data in borehole USW SD-9 from DTN: LAJF831222AQ98.011 [DIRS 145402] are not given. There are two points; one point from perched water and another from the water table. The water table elevation is at SD-9 is given in DTN: MO0106RIB00038.001 [DIRS 155631]. The depth of perched water can be estimated from drilling logs. The perched water sample for SD-9 in DTN: LAJF831222AQ98.011 [DIRS 145402] is identified with the designator SPC00503689. This designator is identified in the sample collection report (Chornack and Soeder, 1994 [DIRS 185766]) as being taken on July 14, 1994. The drilling logs near this date are given in records (Lindsey et al. 1994 [DIRS 185767], p. 113) and Neubauer et al. 1994 [DIRS 185768], p. 1). On July 7, 1994, the perched water depth was identified in the log as being at 1492 feet. On July 13, 1994, the perched water depth was identified in the log as being at 1446.5 feet. Therefore, the average perched water depth is 1469.25 feet. The original analysis used a depth of 1470.08 feet. Given the fact that perched water flows into the borehole from some depth in the formation that cannot be determined exactly, the value used in the original analysis is considered adequate.

The three chloride data points from borehole USW SD-9 given in DTN: GS020408312272.003 [DIRS 160899] were assigned incorrect elevations in the original analysis. The elevations for two of the three data points changed by 10 m or less, which is small compared with the 540 m range of chloride sample elevations for USW SD-9. The third chloride data point moved from below the water table into the UZ, so this adds one chloride data point to the analysis. The effects of these changes on weighting factors were found to be negligible.

J3.6 Re-Analysis of Chloride

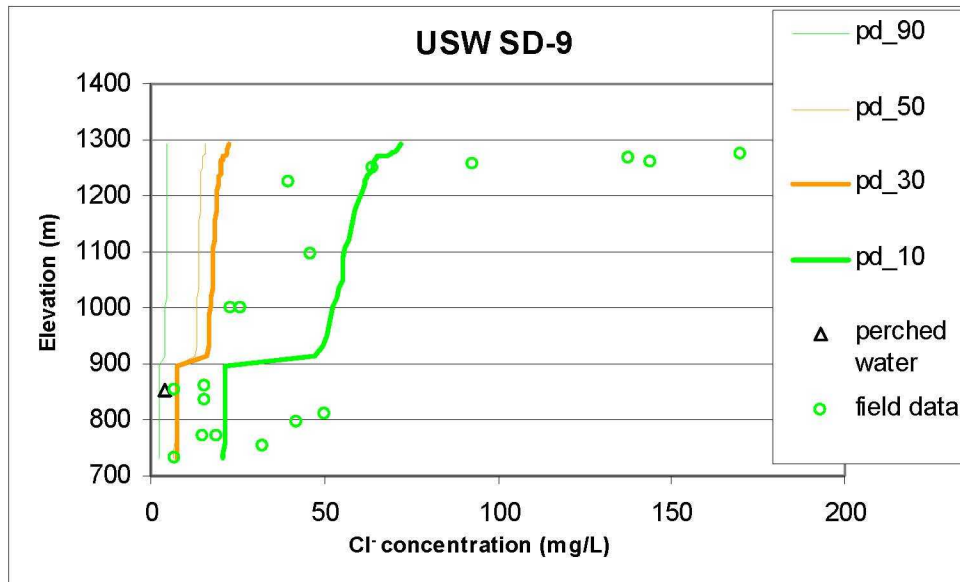
During the course of investigation for CR-11715, it was determined that Figures 6.5-3 and 6.5-4 of the parent report show incorrect source DTN information; DTN: GS020408312272.003 [DIRS 160899] should be removed from the list of data plotted in these figures. Similarly, DTN: GS981008312272.004 [DIRS 153677] should be removed from the list of data plotted for Figure 6.5-7. The plots of chloride data and model results in Figures 6.5-7, 6.5-3, and 6.5-1 have some erroneous field data points, and are replotted in Figures J-15, J-16, and J-17, respectively.



Source DTNs: GS961108312271.002 [DIRS 121708]; GS010708312272.002 [DIRS 156375]; LAJF831222AQ98.011 [DIRS 145402]; GS020408312272.003 [DIRS 160899]; Model Results–output DTN: LB0701UZMCLCAL.001.

DTN: LB0804WTMPCGL.000

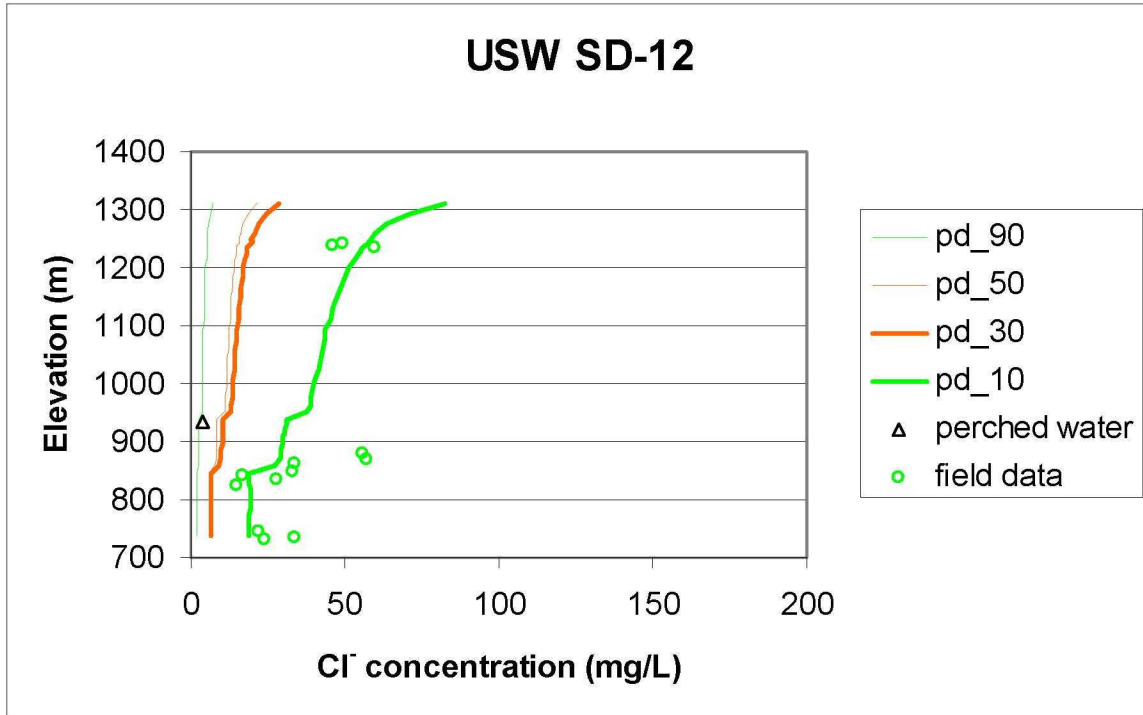
Figure J-15. Chloride Concentration (mg/L) Profiles at Borehole USW NRG-7a for Present-Day 10th, 30th, 50th, and 90th Percentile Infiltrations



Source DTNs: GS970908312271.003 [DIRS 111467]; GS961108312271.002 [DIRS 121708]; LAJF831222AQ98.011 [DIRS 145402]; GS020408312272.003 [DIRS 160899]; Model Results–Output DTN: LB0701UZMCLCAL.001.

DTN: LB0804WTMPCGL.000

Figure J-16. Chloride Concentration (mg/L) Profiles at Borehole USW SD-9 for Present-Day 10th, 30th, 50th, and 90th Percentile Infiltrations

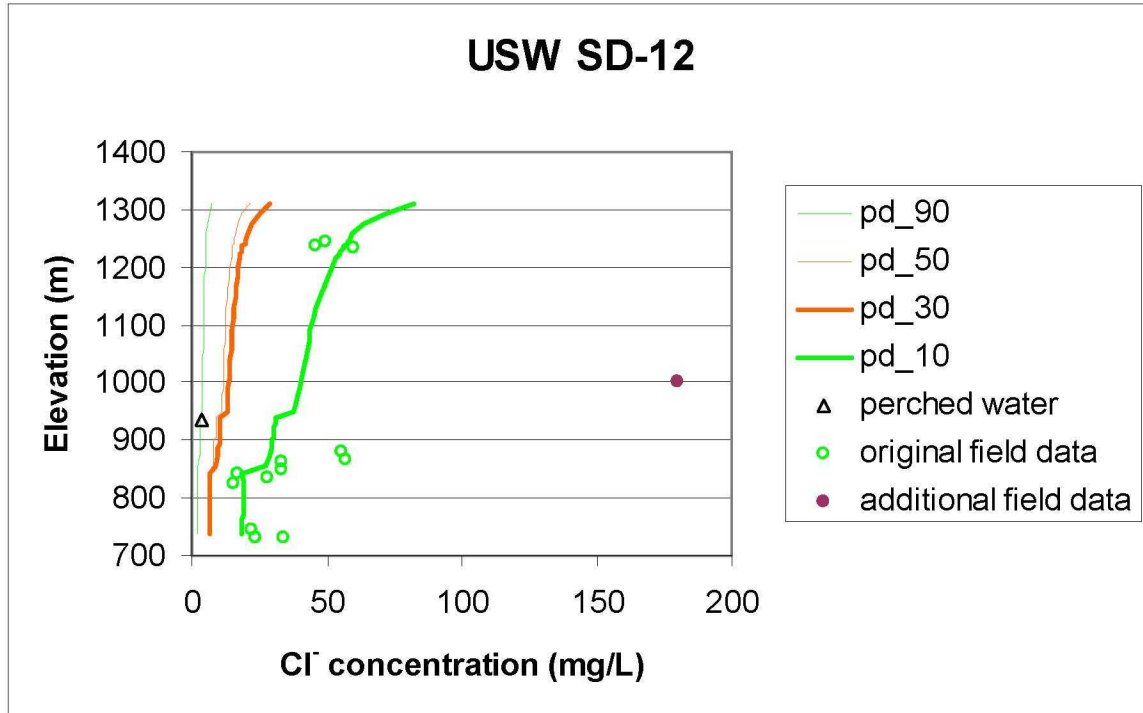


Source DTNs: GS000608312271.001 [DIRS 153407]; GS970908312271.003 [DIRS 111467];
 GS961108312271.002 [DIRS 121708]; GS981008312272.004 [DIRS 153677] Model Results–
 Output DTN: LB0701UZMCLCAL.001.

DTN: LB0804WTMPCLGL.000

Figure J-17. Chloride Concentration (mg/L) Profiles at Borehole USW SD-12 for Present-Day 10th, 30th, 50th, and 90th Percentile Infiltrations

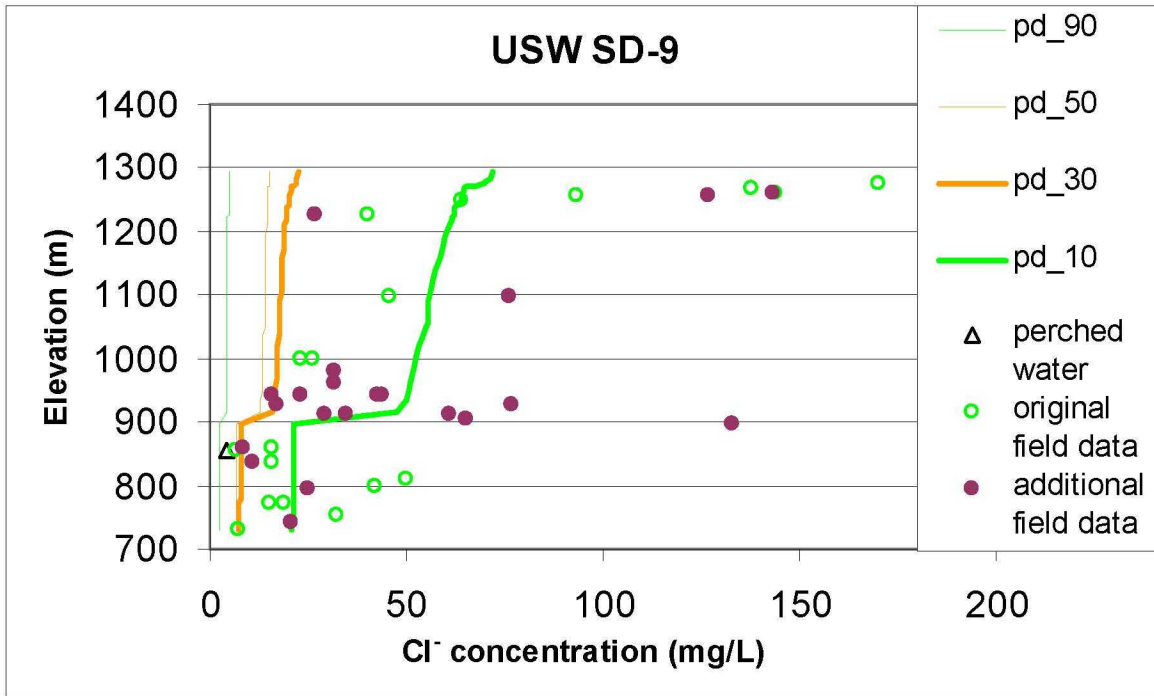
Figures J-18 through J-23 are plotted here to display the additional data not shown on Figures 6.5-1, 6.5-3, 6.5-4, 6.5-5, 6.5-7, and 6.5-10 respectively of the main report. The computed chloride levels from the model (pd_10, pd_30, pd_50, and pd_90) have not changed.



Source DTNs: original field data: GS000608312271.001 [DIRS 153407]; GS970908312271.003 [DIRS 111467]; GS961108312271.002 [DIRS 121708]; GS981008312272.004 [DIRS 153677]; additional field data: GS041108312272.005 [DIRS 178057]. Output DTN: LB0701UZMCLCAL.001.

DTN: LB0804WTMPCGL.000

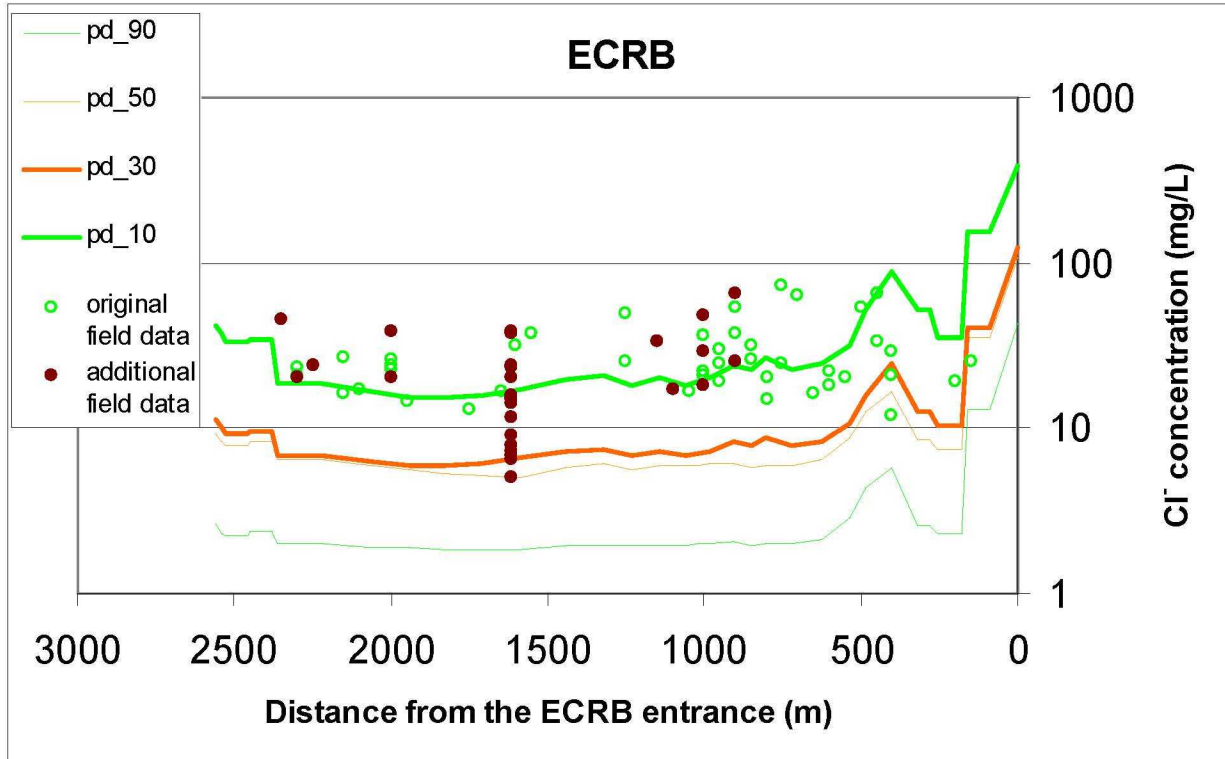
Figure J-18. Chloride Concentration (mg/L) Profiles at Borehole USW SD-12 for Present-Day 10th, 30th, 50th, and 90th Percentile Infiltrations



Source DTNs: original field data: GS970908312271.003 [DIRS 111467]; GS961108312271.002 [DIRS 121708]; LAJF831222AQ98.011 [DIRS 145402]; GS020408312272.003 [DIRS 160899]; additional field data; GS030408312272.002 [DIRS 165226]; GS031008312272.008 [DIRS 166570]; GS041108312272.005 [DIRS 178057]; GS060908312272.004 [DIRS 179065]; GS020808312272.004 [DIRS 166569]. Model Results-Output DTN: LB0701UZMCLCAL.001.

DTN: LB0804WTMPCGL.000

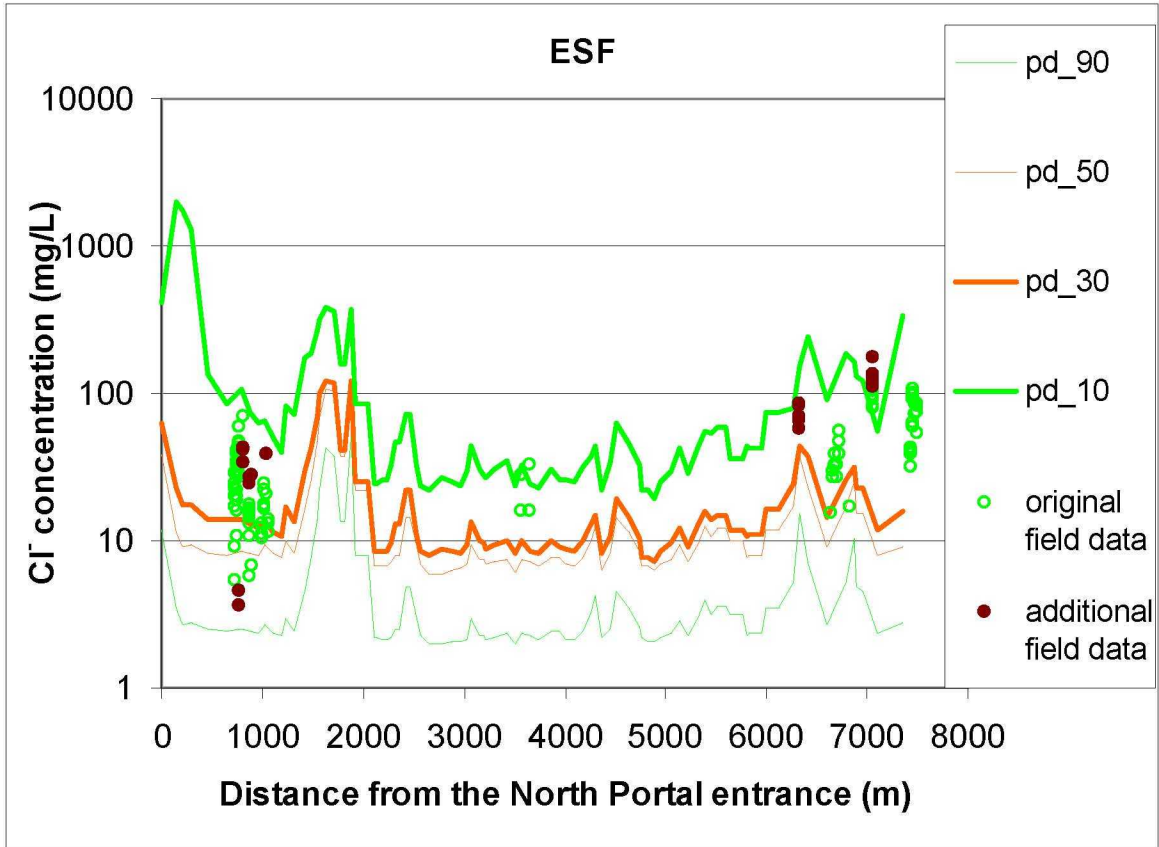
Figure J-19. Chloride Concentration (mg/L) Profiles at Borehole USW SD-9 for Present-Day 10th, 30th, 50th, and 90th Percentile Infiltrations



Source DTNs: original field data: LA9909JF831222.004 [DIRS 145598]; LA0002JF12213U.002 [DIRS 156281]; GS020408312272.003 [DIRS 160899]; additional field data: GS030408312272.002 [DIRS 165226]; GS031008312272.008 [DIRS 166570]; GS020808312272.004 [DIRS 166569]; GS0703PA312272.001 [DIRS 182478]. Model Results—output DTN: LB0701UZMCLCAL.001.

DTN: LB0804WTMPCGL.000

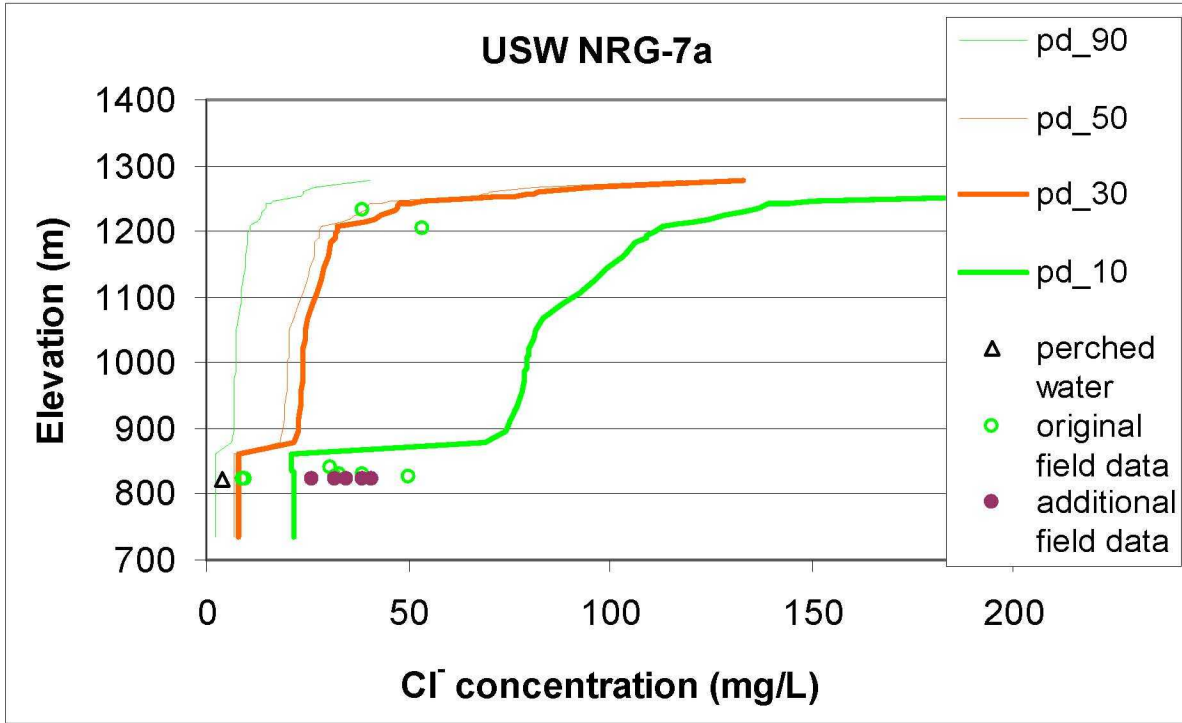
Figure J-20. Chloride Concentration (mg/L) Profiles at the ECRB for Present-Day 10th, 30th, 50th, and 90th Percentile Infiltrations



Source DTNs: original field data: GS961108312261.006 [DIRS 107293]; LA0002JF12213U.002 [DIRS 156281]; LA9909JF831222.010 [DIRS 122733]; additional field data: GS020808312272.004 [DIRS 166569]; GS031008312272.008 [DIRS 166570]. Model Results–Output DTN: LB0701UZMCLCAL.001.

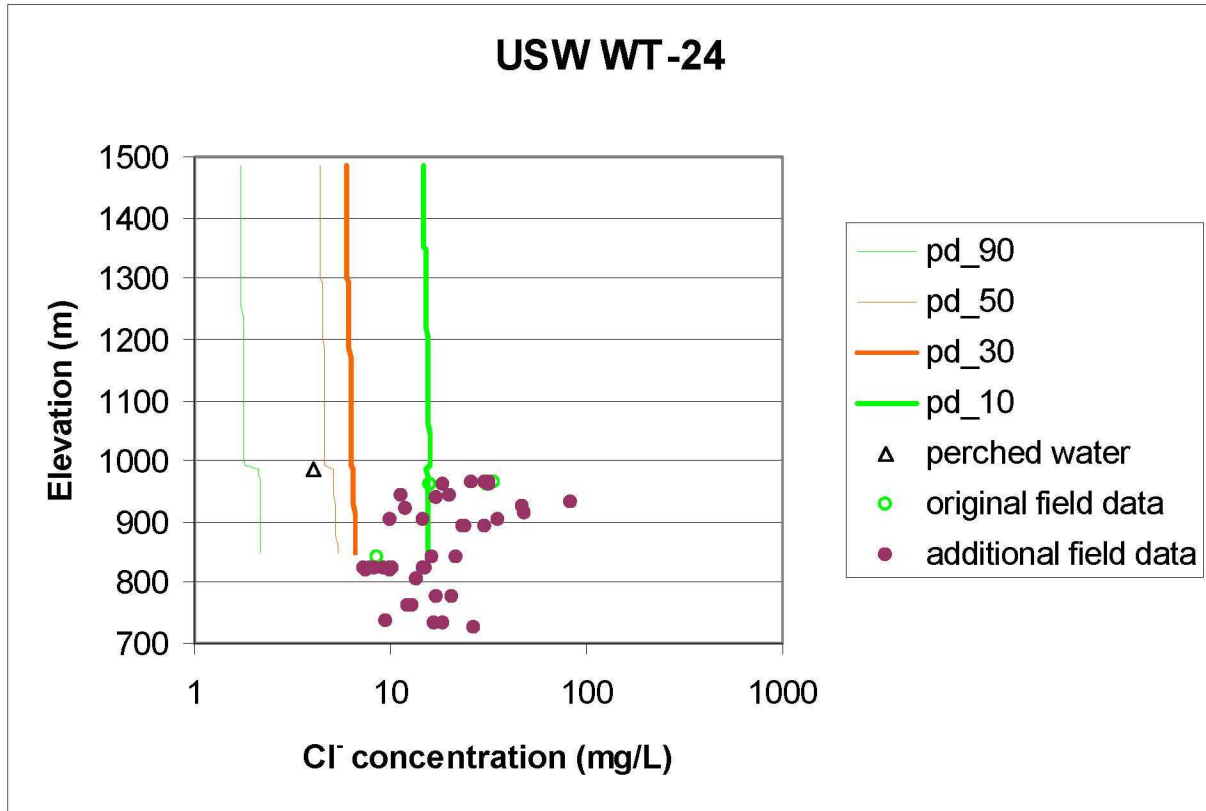
DTN: LB0804WTMPCGL.000

Figure J-21. Chloride Concentration (mg/L) Profiles at the ESF for Present-Day 10th, 30th, 50th, and 90th Percentile Infiltrations



Source DTNs original field data: GS961108312271.002 [DIRS 121708]; GS010708312272.002 [DIRS 156375]; LAJF831222AQ98.011 [DIRS 145402]; GS020408312272.003 [DIRS 160899]; additional field data: GS020808312272.004 [DIRS 166569]. Model Results—output DTN: LB0701UZMCLCAL.001.
DTN: LB0804WTMPCLGL.000

Figure J-22. Chloride Concentration (mg/L) Profiles at Borehole USW NRG-7a for Present-Day 10th, 30th, 50th, and 90th Percentile Infiltrations



Source DTNs: original field data: GS981008312272.004 [DIRS 153677]; LAJF831222AQ98.011 [DIRS 145402];
 additional field data: GS011008312272_004 [DIRS 165859] Model Results–output DTN:
 LB0701UZMCLCAL.001.

DTN: LB0804WTMPCGL.000

Figure J-23. Chloride Concentration (mg/L) Profiles at Borehole USW WT-24 for Present-Day 10th, 30th, 50th, and 90th Percentile Infiltrations

Table J-4 shows the average chloride residuals for each uncertainty case and each borehole or tunnel. As can be seen, at each location the minimum residual occurs for the same uncertainty cases as given in Table 6.5-3 of the main report.

Table J-4. Residual Chloride Concentration in Boreholes and Facilities

Borehole or Facilities	Number of Samples	10th Percentile ^a	30th Percentile	50th Percentile	90th Percentile
G-2	1	0.25	0.13 ^b	0.24	0.58
NRG-6	13	0.23 ^b	0.58	0.73	1.26
NRG-7a	12	0.27 ^b	0.44	0.48	0.93
SD-12	15	0.16 ^b	0.59	0.66	1.14
SD-6	27	0.40 ^b	0.80	0.88	1.32
SD-7	10	0.30 ^b	0.65	0.74	1.18
SD-9	42	0.28 ^b	0.51	0.61	1.10
UZ-14	71	0.32	0.30 ^b	0.31	0.68
UZ-16	44	0.85	0.19 ^b	0.22	0.65
WT-24	19	0.25 ^b	0.58	0.68	1.06
UZ-7a	3	0.28 ^b	0.85	0.97	1.49
UZ-N55	6	0.44 ^b	0.46	0.64	1.17
ESF	40	0.56	0.32 ^b	0.45	0.94
ECRB	32	0.20 ^b	0.48	0.56	1.02

DTN: LB0804WTMPCLGL.000.

^a Percentile infiltration map of present-day climate.

^b Minimum percentile case.

NOTE: Residual concentration represents the absolute difference between calculated and measured chloride concentration (mg/L, in log scale). Minimum residual cases highlighted in yellow.

J3.7 Changes in Weighting Factors

Using the revised temperature and chloride calculations, the weighting factors have been recomputed using the same methodology as described in Section 6.8 of the main report. The previous ambient thermal model results were replaced by the new ambient thermal model results in the existing GLUE analysis spreadsheets for temperature available from the output DTN: LB0701PAWFNFM.001 (files: Cal_t1.xls, Cal_t2_average1.xls, Cal_t2_average2.xls, Cal_t3_average1.xls, Cal_t3_average2.xls, Cal_t4_sum.xls, Cal_t4_sen.xls, Cal_t4_mul.xls; see also Section 6.8 of the main report. Similarly, the additional chloride data were added to the existing GLUE analysis spreadsheets for chloride available from the output DTN: LB0701PAWFNFM.001 (files: Cal_c1.xls, Cal_c2_average1.xls, Cal_c2_average2.xls, Cal_c3_average1.xls, Cal_c3_average2.xls, Cal_c4.xls, Cal_c4_sen.xls, ECRB.xls, ESF.xls, SD-9.xls; see also Section 6.8 of the main report. The results are shown in Table J-5 when considering both changes for ambient thermal model results and the additional chloride data. This table corresponds to Table 6.8-1 of the main report. The weighting factors considering chloride only are given in Table J-6, which corresponds to Table 6.8-4 of the main report. The weighting factors considering temperature only are given in Table J-7, which corresponds to Table 6.8-5 of the main report.

Table J-5. Weighting Factors Considering Both Temperature and Chloride

Infiltration Map	10%	30%	50%	90%
S1	100%	0%	0%	0%
s2_a1_n=1	52%	20%	28%	1%
s2_a1_n=0.5	37%	23%	34%	5%
s2_a2_n=1	43%	20%	36%	1%
s2_a2_n=0.5	33%	23%	38%	6%
s3_a1	96%	4%	0%	0%
s3_a2	97%	3%	0%	0%
s4_sum	26%	24%	32%	17%
Average	61%	15%	21%	4%
Previous average*	62%	16%	16%	6%

DTN: LB0804WTMPCLGL.000.

* Previous average from Table 6.8-1 of the main report.

NOTE: The sum of percentages over the 10% through 90% cases does not necessarily add to 100 because of round-off.

Table J-6. Weighting Factors Considering Chloride Only

Infiltration Map	10%	30%	50%	90%
S1	100%	0%	0%	0%
s2_a1_n=1	51%	22%	21%	6%
s2_a1_n=0.5	35%	23%	27%	15%
s2_a2_n=1	44%	24%	24%	8%
s2_a2_n=0.5	32%	23%	29%	16%
s3_a1	80%	14%	6%	0%
s3_a2	71%	19%	9%	0%
s4_sum	24%	23%	32%	20%
Average	55%	19%	18%	8%
Previous average*	51%	22%	19%	8%

DTN: LB0804WTMPCLGL.000.

* Previous average from Table 6.8-4 of the main report.

NOTE: The sum of percentages over the 10% through 90% cases does not necessarily add to 100 because of round-off.

Table J-7. Weighting Factors Considering Temperature Only

Infiltration Map	10%	30%	50%	90%
S1	100%	0%	0%	0%
s2_a1_n=1	25%	22%	49%	5%
s2_a1_n=0.5	24%	23%	41%	13%
s2_a2_n=1	23%	19%	53%	5%
s2_a2_n=0.5	23%	21%	43%	13%
s3_a1	82%	16%	2%	0%
s3_a2	87%	10%	3%	0%
s4_sum	22%	21%	31%	26%
Average	48%	17%	28%	8%
Previous average*	50%	15%	21%	14%

DTN: LB0804WTMPCLGL.000.

*Previous average from Table 6.8-5 of the main report.

NOTE: The sum of percentages over the 10% through 90% cases does not necessarily add to 100 because of round-off.

To evaluate the impact of these changes, note that for present-day climate, the average infiltration rates are 3.03, 7.96, 12.28, and 26.78 mm/yr for the 10th, 30th, 50th, and 90th percentile infiltration maps, respectively (see Table 6.1-2 of the main report). The mean and standard deviations for present-day infiltration are 6.7 and 6.1 mm/yr, respectively, using the baseline (previous average) weighting factors from Table J-5 and 6.6 and 5.6 mm/yr, respectively, using the sensitivity results (average case) weighting factors from Table J-5. These changes are small and the larger values for the baseline case are conservative relative to the sensitivity case.

APPENDIX K
CR 11762 EVALUATION

K1 Background Information for CR-11762

The UZ flow analyses of chloride data in the main report support the development of weighting factors for the UZ flow uncertainties cases. These weighting factors are used in TSPA. However, the chloride data are shown in the DIRS for the main report as indirect input. The chloride data DTNs are identified in Table 6.5-1 of the main report. These data should be identified as direct input. Of the DTNs identified in this table, only LA0002JF12213U.001 [DIRS 154760] is listed in the TDMS as unqualified. CR-11762 concerns the identification of pore-water chloride data as indirect input when used as direct input for the chloride model and identifies the unqualified status of DTN: LA0002JF12213U.001 [DIRS 154760].

K2 Inputs and/or Software

K2.1 Data

Direct inputs to this error resolution analysis include the following DTNs: GS010708312272.002 [DIRS 156375], GS961108312271.002 [DIRS 121708], GS000608312271.001 [DIRS 153407], GS970908312271.003 [DIRS 111467], GS981008312272.004 [DIRS 153677], and GS990208312272.001 [DIRS 146134]. These DTNs are qualified as shown in the TDMS and linked in the DIRS to the parent report.

During the investigation of this CR, it was also discovered that DTNs containing pore-water chloride data (DTNs: GS030408312272.002 [DIRS 165226] and GS031008312272.008 [DIRS 166570]) were inadvertently not included in the analyses. The evaluation of this additional data is addressed in the analysis for CR-11715 above. Furthermore, pore-water chloride data from DTN: GS020408312272.003 [DIRS 160899], although included in the analyses, were not included in Figure 6.5-3 for chloride levels in borehole SD-9, Figure 6.5-4 for chloride levels in the ECRB, and Figure 6.5-7 for chloride levels in borehole NRG-7a. The corrections for Figures 6.5-3, 6.5-4, and 6.5-7 is given in Figures J-19, J-20, and J-22.

K2.2 Software

No software was used in the evaluation of CR 11762.

K3 Analysis

All the chloride data sets identified in Table 6.5-1 of the main report should be corrected to direct inputs. The descriptions of these data sets, the associated DTNs, and the locations where the data sets were used in the main report are presented in Table J-1 of this document. The unqualified DTN is justified below for the intended use.

All the DTNs in Table 6.5-1 are qualified except LA0002JF12213U.001 [DIRS 154760]. This DTN is a compilation of data from the following DTNs: DTN GS010708312272.002 [DIRS 156375], GS961108312271.002 [DIRS 121708], GS000608312271.001 [DIRS 153407], GS970908312271.003 [DIRS 111467], GS981008312272.004 [DIRS 153677], and GS990208312272.001 [DIRS 146134].

In summary, all the chloride data LA0002JF12213U.001 [DIRS 154760] can be traced back to qualified DTNs which can be used in place of LA0002JF12213U.001 [DIRS 154760] as direct input in the main report. These DTNs are summarized in Table K-1 and are included in Table J-1 as direct inputs. Table K-1 is a correction to and replaces Table 6.5-1 in the main report. This change has no impact on the analyses of chloride data used in the main report.

Table K-1. Chloride Data Sources

Borehole/Facilities	DTN
SD-6	GS981008312272.004 [DIRS 153677]
SD-7	GS000608312271.001 [DIRS 153407] GS970908312271.003 [DIRS 111467] GS961108312271.002 [DIRS 121708] GS981008312272.004 [DIRS 153677] LAJF831222AQ98.011 [DIRS 145402]
SD-9	GS970908312271.003 [DIRS 111467] GS961108312271.002 [DIRS 121708] LAJF831222AQ98.011 [DIRS 145402] GS020408312272.003 [DIRS 160899]
SD-12	GS000608312271.001 [DIRS 153407] GS970908312271.003 [DIRS 111467] GS961108312271.002 [DIRS 121708] GS981008312272.004 [DIRS 153677]
NRG-6	GS010708312272.002 [DIRS 156375] GS961108312271.002 [DIRS 121708] LAJF831222AQ98.011 [DIRS 145402]
NRG-7a	GS961108312271.002 [DIRS 121708] GS010708312272.002 [DIRS 156375] LAJF831222AQ98.011 [DIRS 145402] GS020408312272.003 [DIRS 160899]
UZ-14	GS010708312272.002 [DIRS 156375] GS961108312271.002 [DIRS 121708] GS990208312272.001 [DIRS 146134] LAJF831222AQ98.011 [DIRS 145402]
UZ#16	GS010708312272.002 [DIRS 156375] GS990208312272.001 [DIRS 146134] LAJF831222AQ98.011 [DIRS 145402]
UZ-N55	GS010708312272.002 [DIRS 156375]
UZ-7a	GS981008312272.004 [DIRS 153677]
WT-24	GS981008312272.004 [DIRS 153677] LAJF831222AQ98.011 [DIRS 145402]
G-2	LAJF831222AQ98.011 [DIRS 145402]
ECRB	LA9909JF831222.004 [DIRS 145598] LA0002JF12213U.002 [DIRS 156281] GS020408312272.003 [DIRS 160899]
ESF	GS961108312261.006 [DIRS 107293] LA0002JF12213U.002 [DIRS 156281] LA9909JF831222.010 [DIRS 122733]

APPENDIX L
CR 11796 EVALUATION

L1 Background Information for CR-11796

The following statement is given in Section 6.1.2 of the main report: “The active fracture concept has been evaluated in *Conceptual Model and Numerical Approaches for Unsaturated Zone Flow and Transport* (BSC 2004 [DIRS 170035]) and further sensitivity analyses are provided in Section 6.8.” The sensitivity analyses is not provided in Section 6.8 of BSC (2004) [DIRS 170035], but rather, is provided in Section 6.8 of BSC (2004) [DIRS 169861]. CR- 11796 concerns this erroneous cross-reference that should have been a reference to Section 6.8 of BSC (2004) [DIRS 169861].

L2 Inputs and/or Software

No direct inputs or software were used in the evaluation of CR 11796.

L3 Analysis

A sensitivity study of impact of the active-fracture-model parameter on distributions of matrix water saturation and water potential, percolation flux through repository layers, and tracer transport in the UZ is documented in Section 6.8 in Revision 02 of *UZ Flow Models and Submodels* (BSC 2004 [DIRS 169861]). The statement in Section 6.1.2 of the main report should be corrected to “The active fracture concept has been evaluated in *Conceptual Model and Numerical Approaches for Unsaturated Zone Flow and Transport* (BSC 2004 [DIRS 170035]), and further sensitivity analyses are provided in Section 6.8 in Revision 02 of this report (BSC 2004 [DIRS 169861]).”

During the course of this investigation, an additional reference was also found that requires a correction. In Section 6.8.5.1, third paragraph, second sentence, the reference to “SNL 2007 [DIRS 174294], Figure 6.5.7.1-4”, should be changed to “SNL 2008 [DIRS 182145], Section 8.1[a]”.

APPENDIX M
CR 12866 EVALUATION

M1 Background Information for CR-12866

A direct input in the main report, DTN: LB0210THRMLPRP.001 [DIRS 160799], that is product output of a superseded report, BSC 2003 [DIRS 161773], was not justified for intended use as required by the procedure in effect at the time, SCI-PRO-006 REV 05. CR-12866 concerns this missing justification.

M2 Inputs and/or Software

No direct inputs or controlled software were used in the evaluation of CR 12866. Standard spreadsheets and graphical display using Microsoft ® Excel 2003 documented according to SCI-PRO-006.

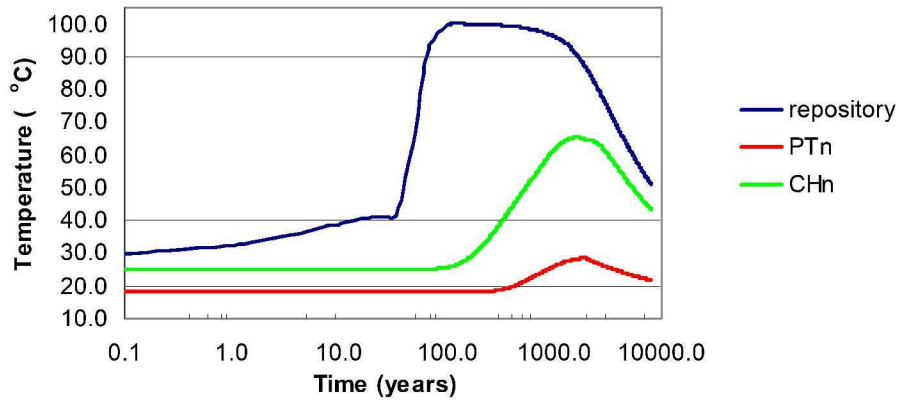
M3 Analysis

The DTN: LB0210THRMLPRP.001 [DIRS 160799] contains thermal properties (wet and dry thermal conductivities) that affect the analysis of steady-state temperatures in the unsaturated zone as evaluated in Section 6.3 of the main report. A revised set of thermal properties are available from DTN: LB0402THRMLPRP.001 [DIRS 168481], however DTN: LB0210THRMLPRP.001 [DIRS 160799] was used. As discussed in CR-12866, DTN: LB0210THRMLPRP.001 [DIRS 160799] was used as direct input without providing justification as required at the time of use in the main report.

The effects of the revised set of thermal properties on mountain-scale thermal-hydrologic processes are documented in *Mountain-Scale Coupled Processes (TH/THC/THM) Models* (BSC 2005 [DIRS 174101]). Appendix V of *Mountain-Scale Coupled Processes (TH/THC/THM) Models* (BSC 2005 [DIRS 174101]) concludes that the differences in thermal properties have little impact on the conclusions drawn from simulation results for mountain-scale thermal hydrological processes. This is based on a variety of comparisons in *Mountain-Scale Coupled Processes (TH/THC/THM) Models* (BSC 2005 [DIRS 174101]) for temperature distributions using both property sets showing nearly identical results: (1) at the repository horizon at 100 years following waste emplacement (Figures 6.3.1-1a and V-1, BSC 2005 [DIRS 174101]); (2) temperature distribution at the repository horizon at 1000 years following waste emplacement (Figures 6.3.1-3a and V-2, BSC 2005 [DIRS 174101]); (3) temperature distribution in a north-south cross-section 1000 years following waste emplacement (Figures 6.3.1-3d and V-3, BSC 2005 [DIRS 174101]); (4) vertical temperature distributions along two columns over a range of times (10 to 2000 years) at locations in the north-central repository area and the southern repository area (Figures 6.3.1-6 and V-4, BSC 2005 [DIRS 174101]); (5) time-temperature histories at three locations from 0.1 to 10,000 years (Figures 6.3.1-7 and V-5, BSC 2005 [DIRS 174101]). Therefore, DTN: LB0210THRMLPRP.001 [DIRS 160799] is suitable for the calculation of ambient, mountain-scale temperatures that are used in the evaluation of effects of infiltration on temperature profiles in the main report.

Note that there is a small discrepancy in the temperature plots at the repository for Figure 6.3.1-7 (BSC 2005 [DIRS 174101]) (reproduced here as Figure M-1), which used thermal properties from DTN: LB0210THRMLPRP.001 [DIRS 160799], and Figure V-5 (BSC 2005 [DIRS 174101]) (reproduced here as Figure M-2), which used thermal properties from DTN:

LB0402THRMLPRP.001 [DIRS 168481]. The discrepancy occurs near the time that ventilation is turned off at 50 years, where a sharp temperature rise occurs. The difference in these figures results from a lower time resolution for the data plotted in Figure M-1, which causes the sharp temperature rise to appear to start at an earlier time (prior to 50 years). Figure M-3 below shows data plotted from DTN: LB0310MTSCLTH3.001 [DIRS 170270], using output files GASOBS.DAT_th_v16.out_1.txt, GASOBS.DAT_th_v16.out_2.txt, GASOBS.DAT_th_v16_2.out.txt, GASOBS.DAT_th_v16_3.out_1.txt, GASOBS.DAT_th_v16_3.out_2.txt, and GASOBS.DAT_th_v16_3.out_3.txt. These are the source files for Figure M-1. Figure M-3 is a re-plot of the time-temperature history for the repository cell shown in Figure M-1 using more data points at times near 50 years. Also, the plot stops at 2000 years, corresponding with the duration plotted in Figure M-2. Temperature versus time was extracted from these files for cell DP12h47, which is the repository cell for Column F (column h47 in the model grid, as identified in Table 6.3-1 of *Mountain-Scale Coupled Processes (TH/THC/THM) Models* (BSC 2005 [DIRS 174101])). The time-temperature data for cell DP12h47 in these files contains well over 100,000 points, so not all points are used in the plot below or in Figure 6.3.1-7 (BSC 2005 [DIRS 174101])). At times near 50 years, a higher time resolution in the data is required to resolve the sharp change in slope of the time-temperature curve for the repository cell. Sufficient data is available in the files from DTN: LB0310MTSCLTH3.001 [DIRS 170270] to better resolve the sharp change in the time-temperature profile at 50 years, however, the selected points used for Figure M-1 does not fully resolve this sharp change. The temperature history for the repository cell in Figure M-3 is seen to be essentially the same as the temperature history at the repository in Figure M-2. Therefore, these comparisons support the conclusion that the differences in thermal properties between DTN: LB0210THRMLPRP.001 [DIRS 160799] and DTN: LB0402THRMLPRP.001 [DIRS 168481] has a negligible effect on the calculated temperatures at the mountain scale.

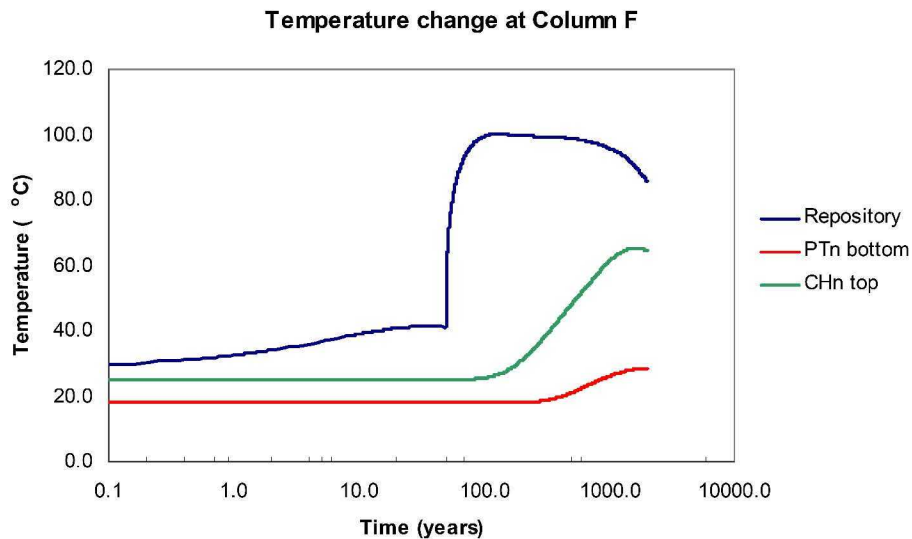


Output DTN: LB0310MTSCLTH3.001.

NOTE: Observation column F is situated in the northern, main repository block center. The bottom of PTn is at an elevation of 1,307.5 m; the top of CHn is at an elevation of 961 m.

Figure 6.3.1-7. Model-Predicted Temperature Changes with Time at Repository Horizon, Bottom PTn, and Top CHn along Observation Column F: Base-Case Model with Ventilation

Figure M-1. (from *Mountain-Scale Coupled Processes (TH/THC/THM) Models* (BSC 2005 [DIRS 174101]))



DTN: LB0404MTSCLTH3.001.

NOTE: Ptn bottom is situated at an elevation of 1,307.5 m; CHn top is situated at an elevation of 961 m; Observation Column F is located in the Northern or Main Repository Block Center. Figure shows base-case model with ventilation, using new estimates of thermal properties.

Figure V-5. Model-Predicted Temperature Changes with Times at Repository Horizon, Bottom PTn, and Top CHn Along the Observation Column F

Figure M-2. (from *Mountain-Scale Coupled Processes (TH/THC/THM) Models* (BSC 2005 [DIRS 174101]))

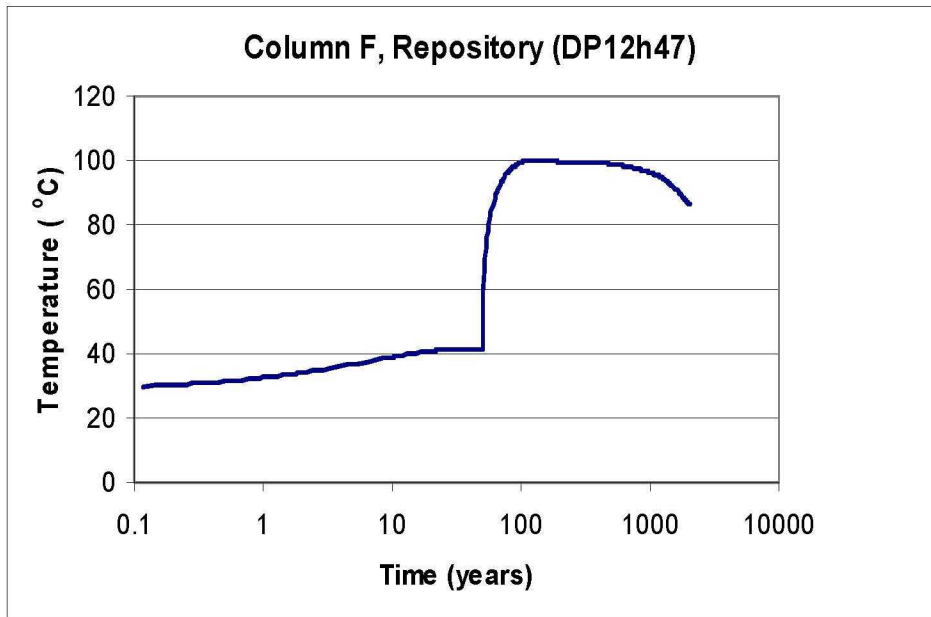


Figure M-3. Re-plot of the time-temperature history given in Figure 6.3.1-7 of *Mountain-Scale Coupled Processes (TH/THC/THM) Models* (BSC 2005 [DIRS 174101]) for the repository for a period from approximately 0.1 years to 2000 years

Impact Evaluations for MDL-NBS-HS-000006 REV03 AD01 ERD04**CR-11715**

CR-11715 concerns the water table temperature used for the ambient thermal model. Calibration of the water table temperatures was performed to optimize the fit of the UZ ambient thermal model under a given infiltration rate. This calibration is inconsistent with the current use of the ambient thermal model as an independent assessment of infiltration rates. A revised water table temperature map was implemented to correct the original water table map that had been calibrated against previous UZ ambient thermal model results. This calibration was not appropriate for the current use of the ambient thermal model, which is to evaluate differences between the ambient thermal model and temperature data given different infiltration map boundary conditions and to arrive at weighting factors based on these comparisons as well as similar comparisons involving chloride data. The new water table temperature map is an interpolation of the existing water table temperature data without any additional calibrations or adjustments. The temperature results were found to be similar, with the minimum residuals between computed and observed temperatures occurring for the same infiltration maps. Additional chloride data, inadvertently left out of the previous analyses, were added to the comparisons of computed and observed chloride concentrations. As for temperature, the results were found to be similar, with the minimum residuals between computed and observed chloride concentrations occurring for the same infiltration maps. The revised GLUE analyses for the infiltration map weighting factors were found to have relatively small changes as a result of the changes in the computed temperatures from the ambient thermal model and the additional chloride data. Changes in average weighting factors are given in Tables J-5, J-6, and J-7. TSPA implements the average weighting factors based on temperature and chloride data. The largest relative change in these average weighting factors occurred for the 50th and 90th percentile cases, where the 50th percentile weighting factor increased and 90th percentile weighting factor decreased. The weighted average present-day infiltration rate using the new weighting factors is 6.6 mm/yr as compared with 6.7 mm/yr using the previous weighting factors. Therefore, the changes in weighting factors are not expected to result in adverse effects on dose predictions in TSPA. The results of simulations conducted in this ERD show that errors identified in this CR do not impact the conclusions of the main report. The revision to Figures 6.5-1, 6.5-3, and 6.5-7 affect Figures 2.3.2-18, 2.3.2-20, and 2.3.2-24 of the Safety Analysis Report. No other changes reported here relative to CR-11715 affect the Safety Analysis Report.

CR-11762

CR-11762 concerns the identification of pore-water chloride data as indirect input when used as direct input for the chloride model and addresses the qualification status of the chloride data used. The use of the unqualified DTN: LA0002JF12213U.001 [DIRS 154760] for chloride concentration data has been evaluated. It was found that all the data presented in this DTN can be traced back to other qualified DTNs. The only change required to address CR-11762 is to replace Table 6.5-1 of the main report with Table K-1. This change has no impact on the analyses of chloride data in this report, TSPA, or on the Safety Analysis Report.

CR-11796

CR- 11796 concerns an erroneous cross-reference that should have been a reference to an external document. The changes for this CR are editorial and have no impact.

CR-12866

CR-12866 concerns the use of thermal properties data associated with a superseded report as direct input, without providing the required justification. Justification for use of a direct input that is product output of a superseded document has been provided. This justification has no impact on the results of the main report, TSPA, or the Safety Analysis Report.

Other documents linked to UZ Flow Models and Submodels are listed below:

1. 800-IED-MGR0-00401-000 Rev. 00J, *IED Geotechnical and Thermal Parameters*
2. ANL-WIS-MD-000024 Rev. 01, *Postclosure Nuclear Safety Design Bases*
3. ANL-WIS-MD-000027 Rev. 00, *Features, Events, and Processes for the Total System Performance Assessment: Analyses*
4. MDL-WIS-PA-000005 Rev. 00, Addendum 01, *Total System Performance Assessment Model/Analysis for the License Application*
5. MDL-WIS-PA-000005 Rev. 00, *Total System Performance Assessment Model/Analysis for the License Application*
6. TDR-NBS-HS-000020 Rev. 00, *Data Qualification Report for Simulation of Net Infiltration for Present Day and Potential Future Climates Preliminary Output*
7. TDR-PCS-SE-000001 Rev. 05, Addendum 01, *Performance Confirmation Plan*
8. DOE/EIS-0250F-S1, *Final Supplemental Environmental Impact Statement for a Geologic Repository for the Disposal of Spent Nuclear Fuel and High-Level Radioactive Waste at Yucca Mountain, Nye County, Nevada*
9. ANL-EBS-PA-000012 Rev. 00 *Postclosure Design Input Parameters for Subsurface Facilities*
10. 800-KMC-SS00-00500-000-00B *VULCAN 6.0 GFM2000 Representation*
11. MDL-NBS-HS-000021 REV 03 AD 02, *Saturated Zone Flow and Transport Model Abstraction.*
12. ANL-EBS-MD-000049 REV 03 ADD 01, *Multiscale Thermohydrologic Model.*

None of the changes or sensitivity analyses presented in this ERD impact these downstream documents.